tinyurl.com/AGVisIEEE20

The Past, Present and Future of Visualization in Astronomy

Alyssa A. Goodman *(and MANY others!)*

Center for Astrophysics | Harvard & Smithsonian, Radcliffe Insitute for Advanced Study, HDSI Steering Committee & glue solutions, inc.

@AlyssaAGoodman

© KIPAC, AMNH

Why have astronomers been obsessed with visualization forever?

Our Universe is not two-dimensional, but the Sky is.

Our Universe is not two-dimensional, but the Sky is.

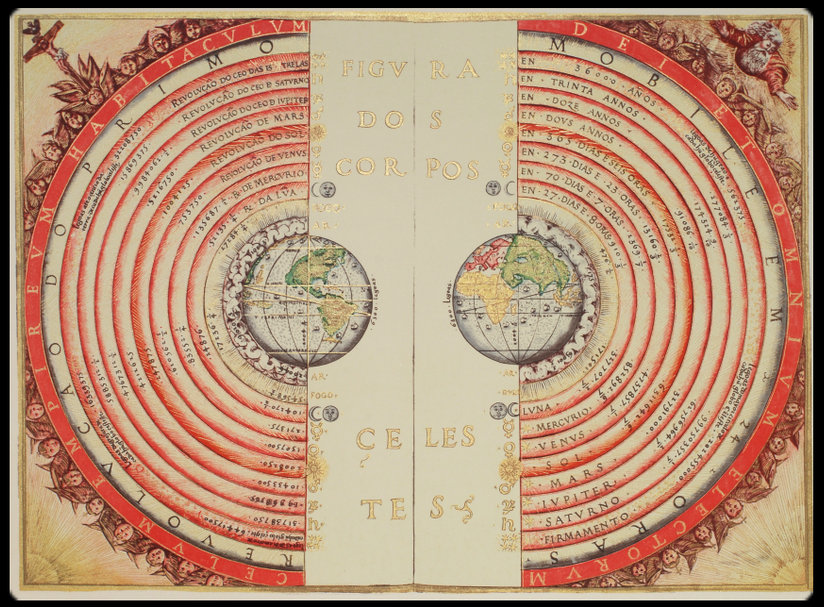

100 AD–16th Century

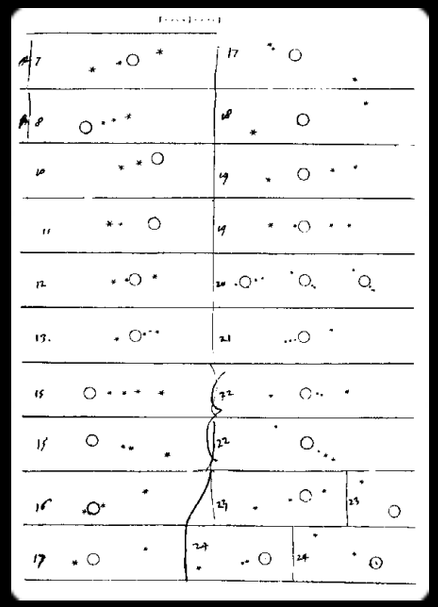

17th Century

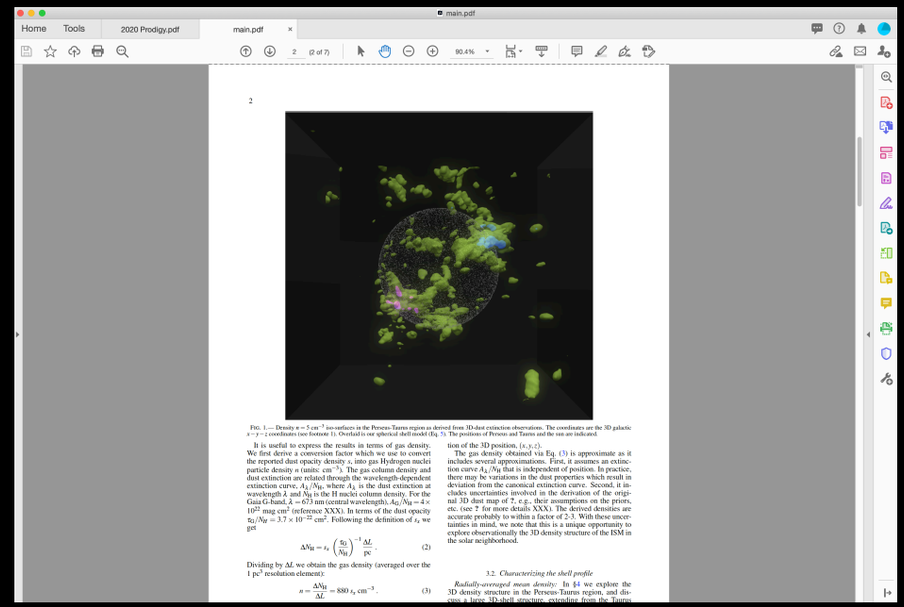

21st Century

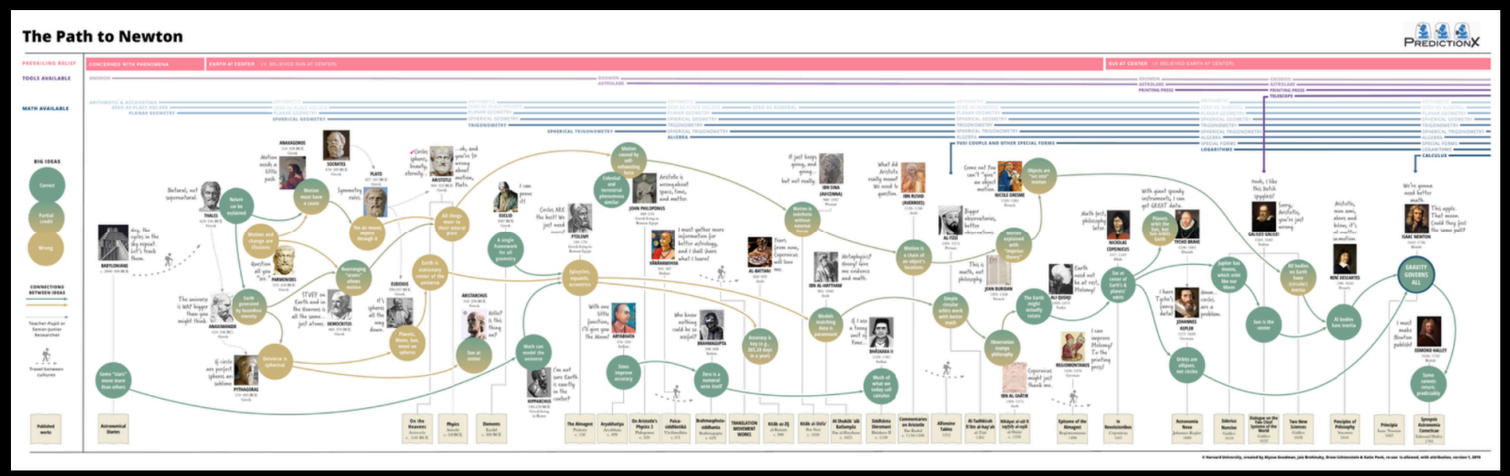

"The Path to Newton"

100 years of Perseus

+2 Challenges...

"case" as a variable...

3D selection

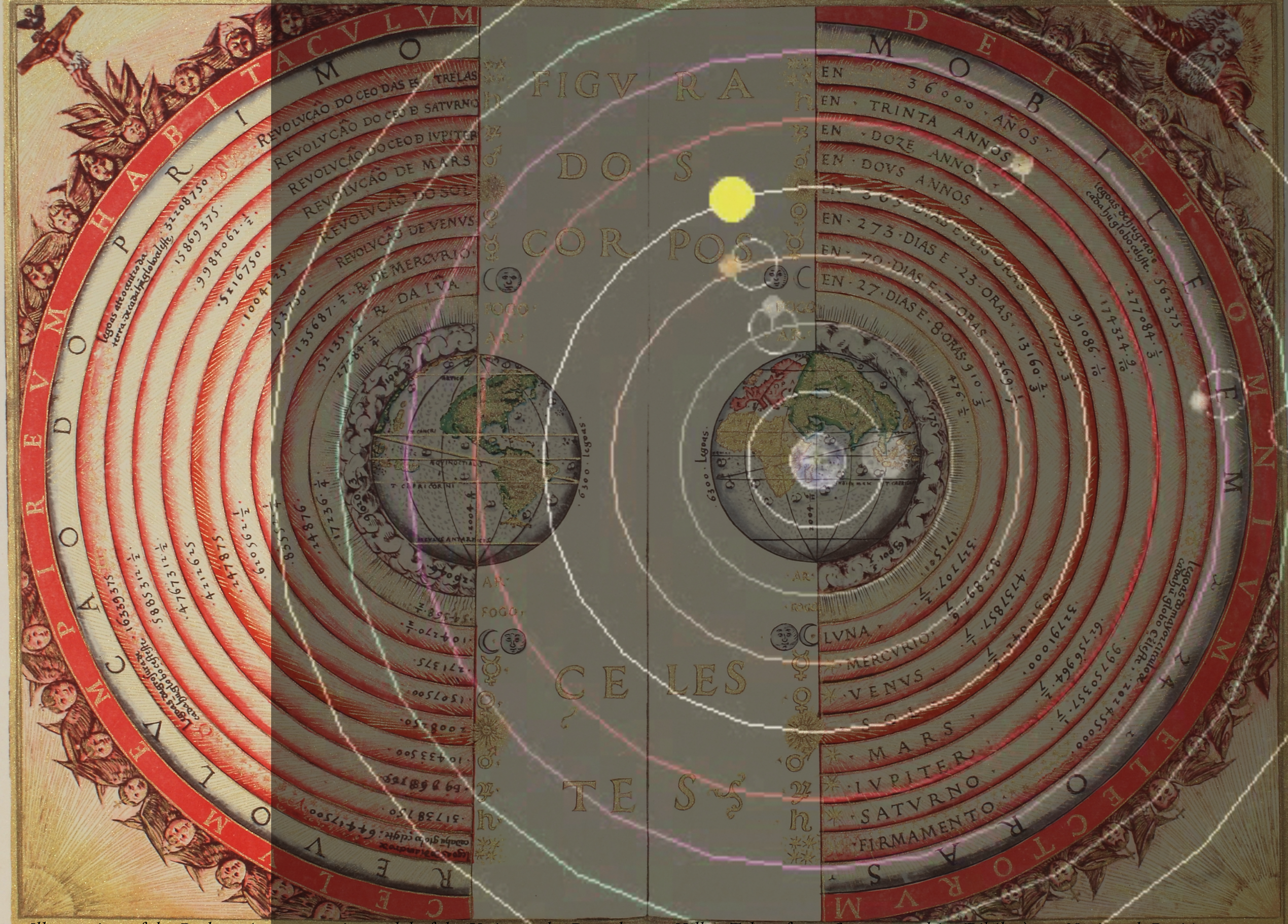

Illustration of the Ptolemaic geocentric model of the Universe by Bartolomeu Velho. Taken from Cosmographia (Bibilotèque National, Paris).

Moon

Mercury

Venus

Sun

Mars

Jupiter

Saturn

The Firmament

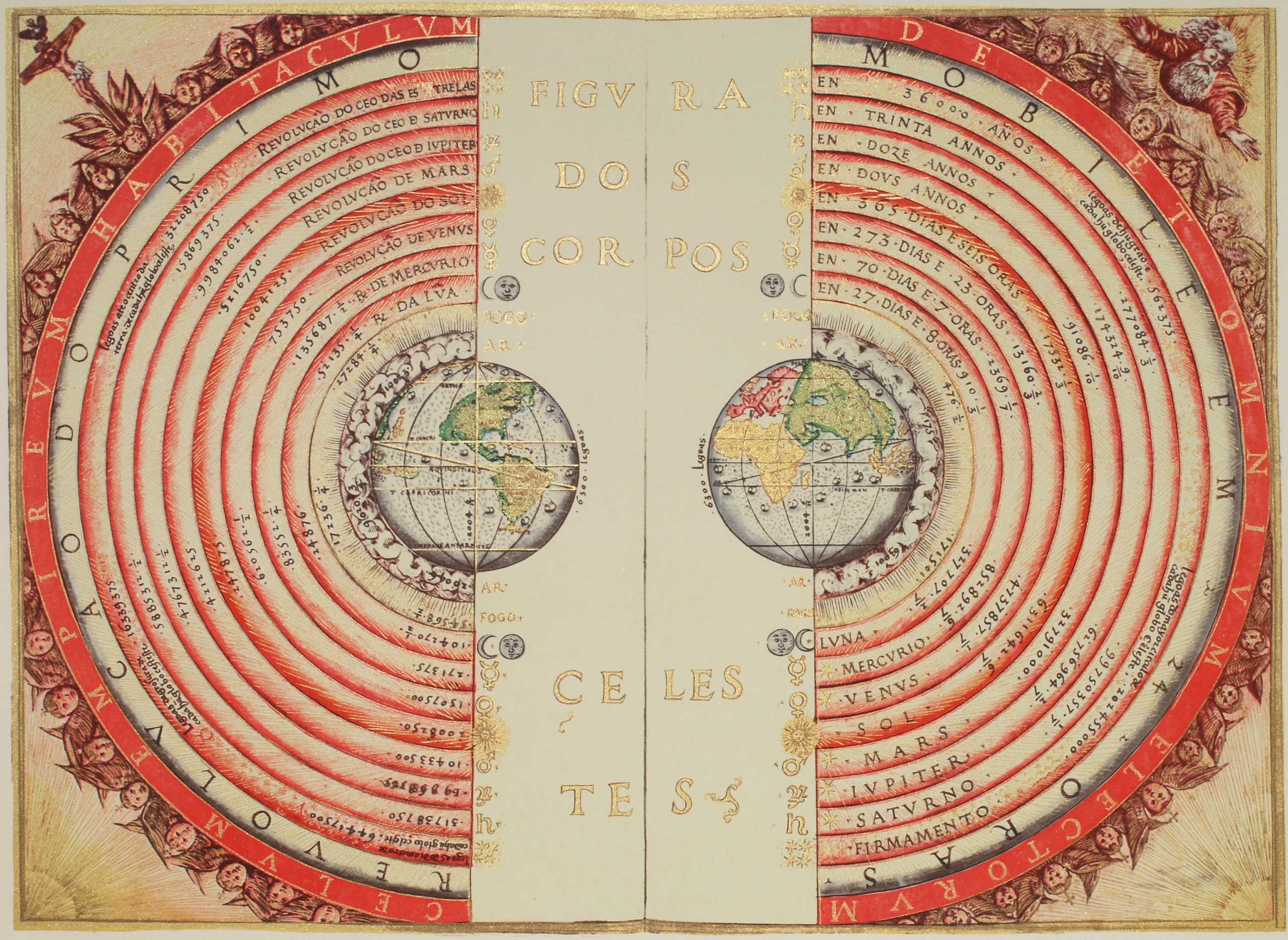
FIGVRA DOS CORPOS CELESTES
MOBILE DE MINVM ELECTORVM
MOBILE DE MINVM ELECTORVM
CELVM PRIOR DE MOVEM
REVOLVÇÃO DO CEO DAS ESTRELAS
REVOLVÇÃO DO CEO D SATVRNO
REVOLVÇÃO DO CEO D IVPITER
REVOLVÇÃO DE MARS
REVOLVÇÃO DO SOL
REVOLVÇÃO DE VENVS
R DE MERCVRIO
R DA LVA
EN 36000 ANOS
EN TRINTA ANNOS
EN DOZE ANNOS
EN DOVS ANNOS
EN 365 DIAS E SEIS ORAS
EN 273 DIAS E 23 ORAS
EN 70 DIAS E 7 ORAS
EN 27 DIAS E 8 ORAS
LVNA
MERCVRIO
VENVS
SOL
MARS
IVPITER
SATVRNO
FIRMAMENTO
FOGO
AR
6300 Legoas

The Firmament	36000 years
Saturn	30 years
Jupiter	12 years
Mars	2 years
Sun	365 Days
Venus	273 Days
Mercury	70 Days
Moon	27 Days

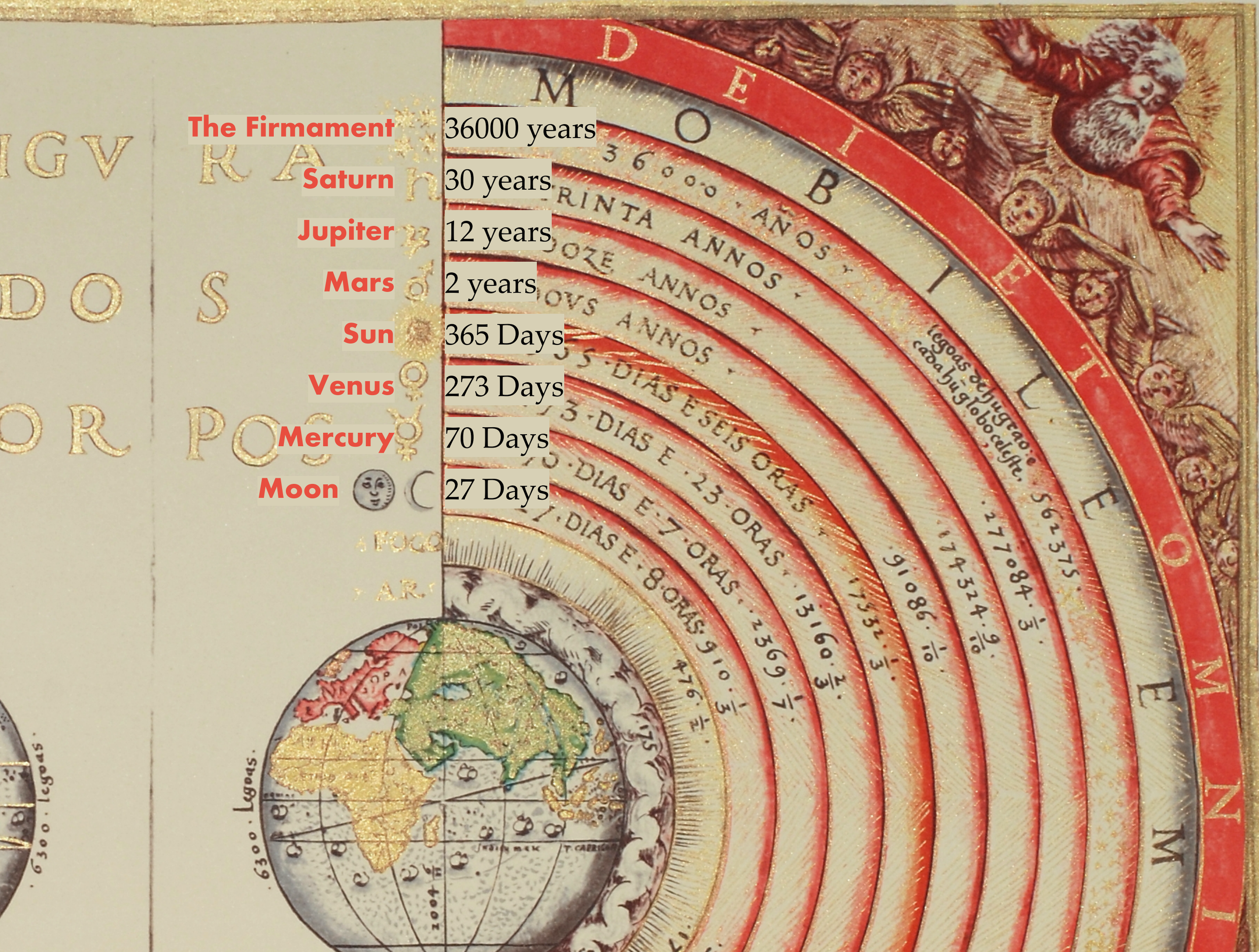

Our Universe is not two-dimensional, but the Sky is.

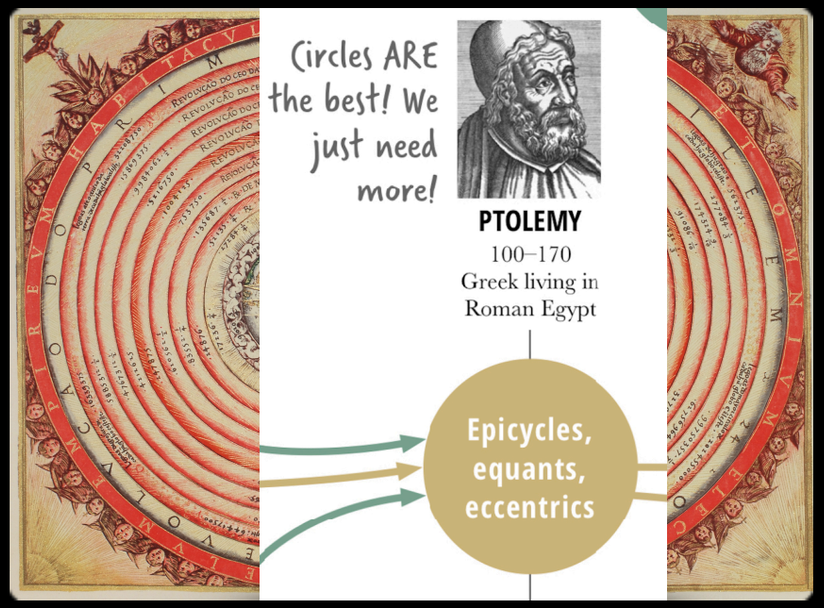

100 AD–16th Century

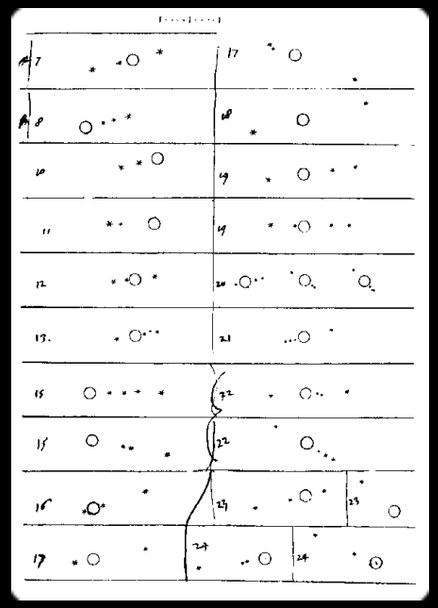

17th Century

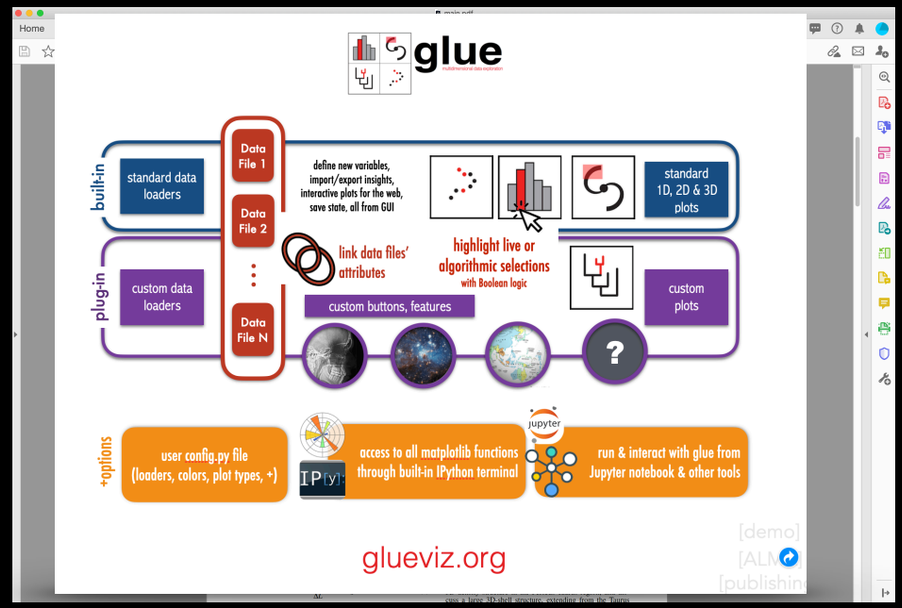

21st Century

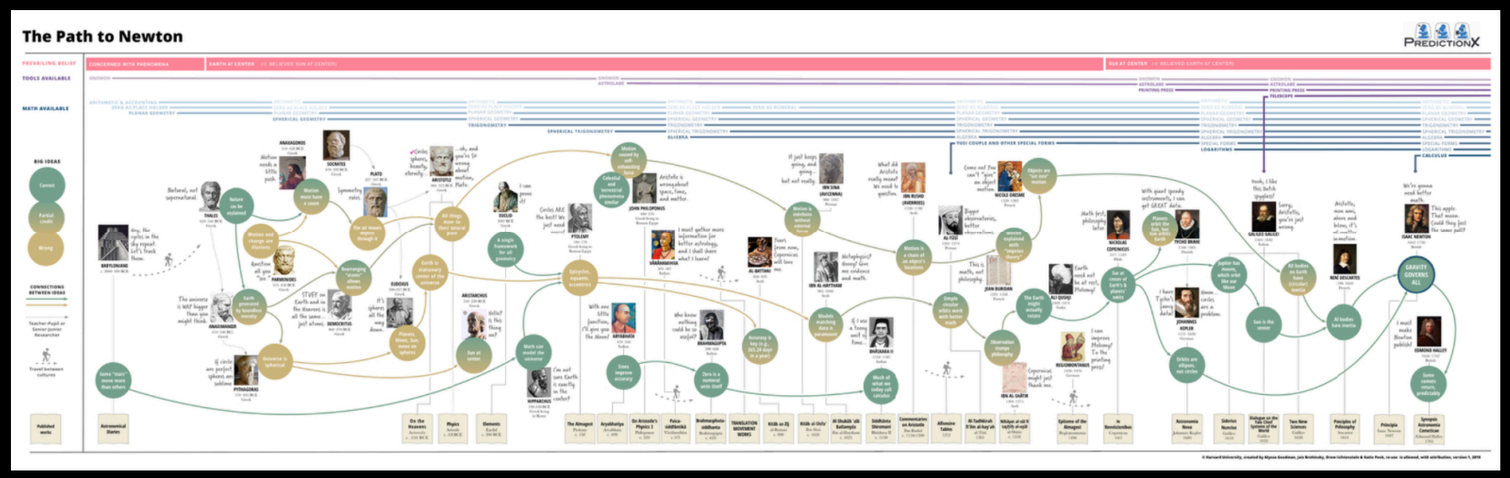

"The Path to Newton"

100 years of Perseus

+2 Challenges...

"case" as a variable...

3D selection

The Path to Newton

PREVAILING BELIEF

CONCERNED WITH PHENOMENA

EARTH AT CENTER (⊙ BELIEVED SUN AT CENTER)

TOOLS AVAILABLE

GNOMON

GNOMON
ASTRO

MATH AVAILABLE

ARITHMETIC & ACCOUNTING
ZERO AS PLACE HOLDER
PLANAR GEOMETRY

ARITHMETIC
ZERO AS PLACE HOLDER
PLANAR GEOMETRY
SPHERICAL GEOMETRY

ARITHMETIC
ZERO AS PLACE HOLDER
PLANAR GEOMETRY
SPHERICAL GEOMETRY
TRIGONOMETRY

SPRERICAL TRIGONOMETRY

BIG IDEAS

Correct

Partial credit

Wrong

CONNECTIONS BETWEEN IDEAS

Teacher-Pupil or Senior-Junior Researcher

Travel between cultures

Published works

Hey, the cycles in the sky repeat. Let's track them.

BABYLONIANS
c. 2000–300 BCE

Some "stars" move more than others

Astronomical Diaries

Natural, not supernatural.

THALES
624–546 BCE
Greek

Nature can be explained

Motion and change are illusions

Question all you "see."

PARMENIDES
515–450 BCE
Greek

Motion needs a little push.

ANAXAGOROS
510–428 BCE
Greek

Motion must have a cause

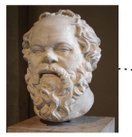

SOCRATES
470–399 BCE
Greek

PLATO
427–347 BCE
Greek

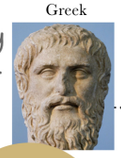

Symmetry rules.

The air moves objects through it

Rearranging "atoms" allows motion

The universe is WAY bigger than you might think.

ANAXIMANDER
610–546 BCE
Greek

Earth generated by boundless eternity

If circles are perfect, spheres are sublime.

PYTHAGORAS
570–495 BCE
Greek

Universe is spherical

STUFF on Earth and in the Heavens is all the same... just atoms.

DEMOCRITUS
460–370 BCE
Greek

It's spheres all the way down.

EUDOXUS
390-337 BCE
Greek

Planets, Moon, Sun, move on spheres

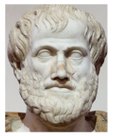

Circles, spheres, beauty, eternity...

ARISTOTLE
383–322 BCE
Greek

...oh, and you're so wrong about motion, Plato.

All things move to their natural place

Earth is stationary center of the universe

On the Heavens
Aristotle
c. 350 BCE

Physics
Aristotle
c. 320 BCE

I can prove it!

EUCLID
300? BCE
Greek

A single framework for all geometry

Elements
Euclid
c. 300 BCE

Circles ARE the best! We just need more!

PTOLEMY
100–170
Greek living in Roman Egypt

Epicycles, equants, eccentrics

The Almagest
Ptolemy
c. 150

With one little function, I'll give you the Moon!

ARISTARCHUS
310–230 BCE
Greek

Hello? Is this thing on?

Sun at center

Math can model the universe

I'm not sure Earth is exactly in the center?

HIPPARCHUS
190-120 BCE
Greek living in Rome

SUN AT CENT

GNOMON
ASTROLABE

ARITHMETIC
ZERO AS PLACE HOLDER
PLANAR GEOMETRY
SPHERICAL GEOMETRY
TRIGONOMETRY
SPHERICAL TRIGONOMETRY
ALGEBRA

ZERO AS NUMERAL

SPRERICAL TRIGONOMETRY

ARITHMETIC
ZERO AS NUMERAL
PLANAR GEOMETRY
SPHERICAL GEOMETRY
TRIGONOMETRY
SPRERICAL TRIGONOMETRY
ALGEBRA

TUSI COUPLE AND OTHER SPECIAL FORMS

Motion caused by self-exhausting force

Celestial and terrestrial phenomena similar

Aristotle is wrong about space, time, and matter.

JOHN PHILOPONUS
490–570
Greek living in Roman Egypt

Circles ARE the best! We just need more!

PTOLEMY
100–170
Greek living in Roman Egypt

I must gather more information for better astrology, and I shall share what I learn!

VĀRĀHAMIHIRA
505–587
Indian

Epicycles, equants, eccentrics

With one little function, I'll give you the Moon!

ARYABHATA
476–550
Indian

Sines improve accuracy

I'm not sure Earth is exactly in the center?

PARCHUS
-120 BCE
ek living
Rome

Who knew nothing could be so useful?

BRAHMAGUPTA
598–668
Indian

Zero is a numeral unto itself

Accuracy is key (e.g., 365.24 days in a year)

Years from now, Copernicus will love me.

AL-BATTANI
858–929
Arab

It just keeps going, and going... but not really.

IBN SINA (AVICENNA)
980–1037
Persian

Motion is indefinite without external forces

Metaphysics? Hooey! Give me evidence and math.

IBN AL-HAYTHAM
965–1040
Arab

Models matching data is paramount

If I use a teeny unit of time...

BHĀSKARA II
1114–1185
Indian

Much of what we today call calculus

What did Aristotle really mean? We need to question.

IBN RUSHD (AVERROES)
1126–1198
Arab

Motion is a chain of an object's locations

Bigger observatories, better observations.

AL-TUSI
1201–1274
Persian

Motion explained with "impetus theory"

Simple circular orbits work with better math

This is math, not philosophy.

JEAN BURIDAN
1295–1358
French

Come on! You can't "give" an object motion.

NICOLE ORESME
1320–1382
French

Objects are "set into" motion

The Earth might actually rotate

Earth need not be at rest, Ptolemy!

ALI QUSHJI
1403–1474
Turkic

Math first, philosophy later.

NICHOLAS COPERNICUS
1473–1543
Polish

Sun at center of Earth's & planets' orbits

I can improve Ptolemy! To the printing press!

REGIOMONTANUS
1436–1476
German

The Almagest
Ptolemy
c. 150

Aryabhatiya
Aryabhata
c. 499

On Aristotle's Physics 3
Philoponus
c. 520

Pañca-siddhāntikā
Vārāhamihira
c. 575

Brahmasphuta-siddhanta
Brahmagupta
c. 628

TRANSLATION MOVEMENT WORKS

Kitāb az-Zīj
al-Battani
c. 900

Kitāb al-Shifa'
Ibn Sīnā
c. 1020

Al-Shukūk 'alā Batlamyūs
Ibn al-Haytham
c. 1025

Siddhānta Shiromani
Bhāskara II
c. 1150

Commentaries on Aristotle
Ibn Rushd
c. 1150-1200

Alfonsine Tables
1252

Al-Tadhkirah fi'ilm al-hay'ah
al-Tusi
1261

Epitome of the Almagest
Regiomontanus
1496

De Revolutionibus
Copernicus
1543

PREDICTIONX

SUN AT CENTER (⊕ BELIEVED EARTH AT CENTER)

GNOMON
ASTROLABE
PRINTING PRESS

ARITHMETIC
ZERO AS NUMERAL
PLANAR GEOMETRY
SPHERICAL GEOMETRY
TRIGONOMETRY
SPRERICAL TRIGONOMETRY
ALGEBRA
TUSI COUPLE AND OTHER SPECIAL FORMS

GNOMON
ASTROLABE
PRINTING PRESS
TELESCOPE

ARITHMETIC
ZERO AS NUMERAL RAL
PLANAR GEOMETRY
SPHERICAL GEOMETRY
TRIGONOMETRY
SPERHICAL TRIGONOMETRY
ALGEBRA
SPECIAL FORMS
LOGARITHMS

ARITHMETIC
ZERO AS NUMERAL
PLANAR GEOMETRY
SPHERICAL GEOMETRY
TRIGONOMETRY
SPHRERICAL TRIGONOMETRY
ALGEBRA
SPECIAL FORMS
LOGARITHMS
CALCULUS

IBN RUSHD (AVERROES)
1126–1198
Arab

Motion is a chain of an object's locations

AL-TUSI
1201–1274
Persian

Bigger observatories, better observations.

Motion explained with "impetus theory"

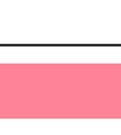

JEAN BURIDAN
1295–1358
French

This is math, not philosophy.

Simple circular orbits work with better math

The Earth might actually rotate

ALI QUSHJI
1403–1474
Turkic

Earth need not be at rest, Ptolemy!

REGIOMONTANUS
1436–1476
German

I can improve Ptolemy! To the printing press!

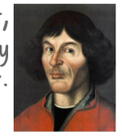

NICHOLAS COPERNICUS
1473–1543
Polish

Math first, philosophy later.

Sun at center of Earth's & planets' orbits

Objects are "set into" motion

NICOLE ORESME
1320–1382
French

Come on! You can't "give" an object motion.

With giant spendy instruments, I can get GREAT data.

Planets orbit the Sun, but Sun orbits Earth

TYCHO BRAHE
1546–1601
Danish

JOHANNES KEPLER
1571–1630
German

I have Tycho's fancy data!

Hmm... circles are a problem.

Orbits are ellipses, not circles

Jupiter has moons, which orbit like our Moon

Sun is the center

GALILEO GALILEI
1564–1642
Italian

Oooh, I like this Dutch spyglass!

Sorry, Aristotle, you're just wrong.

All bodies on Earth have (circular) inertia

All bodies have inertia

Aristotle, mon ami, above and below, it's all matter in motion.

RENÉ DESCARTES
1596–1650
French

GRAVITY GOVERNS ALL

ISAAC NEWTON
1642–1726
British

We're gonna need better math.

This apple. That moon. Could they feel the same pull?

EDMOND HALLEY
1656–1742
British

I must make Newton publish!

Some comets return, predictably

Commentaries on Aristotle
Ibn Rushd
c. 1150-1200

Alfonsine Tables
1252

Al-Tadhkirah fi'ilm al-hay'ah
al-Tusi
1261

Epitome of the Almagest
Regiomontanus
1496

De Revolutionibus
Copernicus
1543

Astronomia Nova
Johannes Kepler
1609

Siderius Nuncius
Galileo
1610

Dialogue on the Two Chief Systems of the World
Galileo
1632

Two New Sciences
Galileo
1638

Principles of Philosophy
Descartes
1644

Principia
Isaac Newton
1687

Synopsis Astronomia Cometicae
Edmond Halley
1705

© Harvard University, created by Alyssa Goodman, Jais Brohinsky, Drew Lichtenstein & Katie Peek, re-use is allowed, with attribution, version 1, 2019

path-to.org

Path to

About Projects Contact

PAT

A project to tr

TRY T

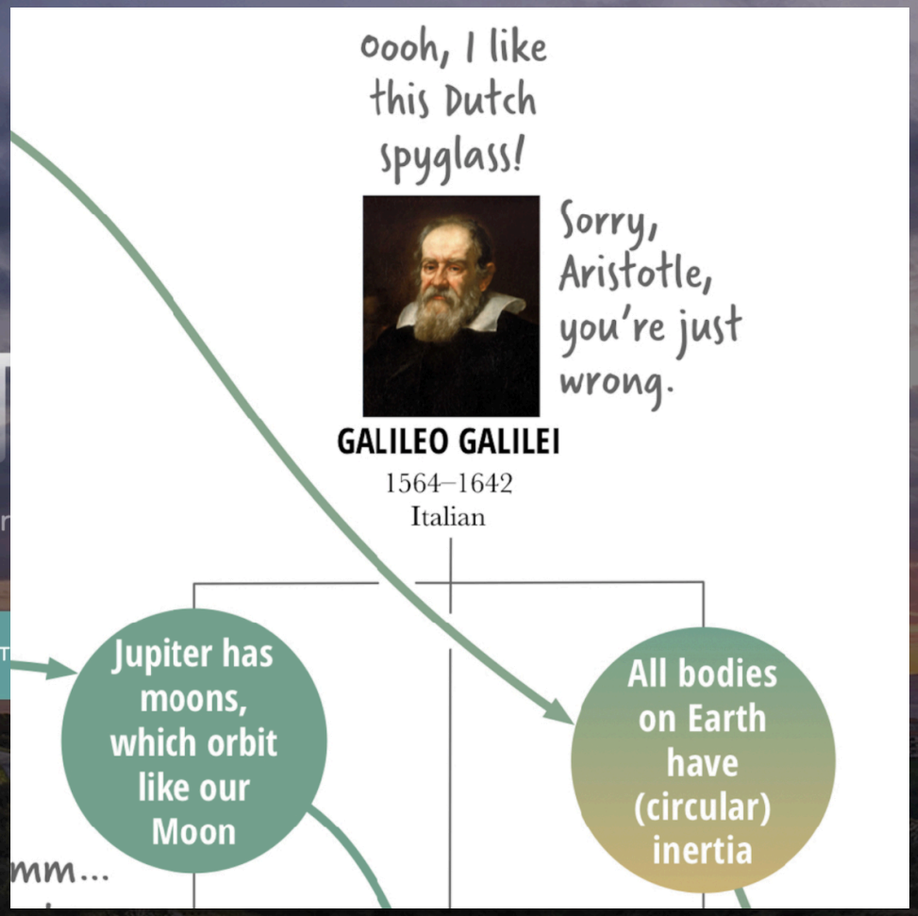

https://path-to.org/newton.html

Our Universe is not two-dimensional, but the Sky is.

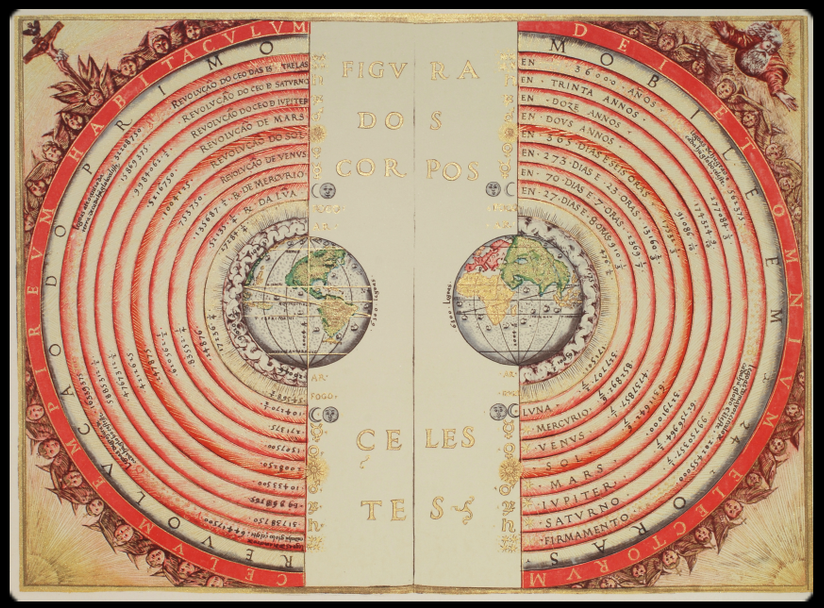

100 AD–16th Century

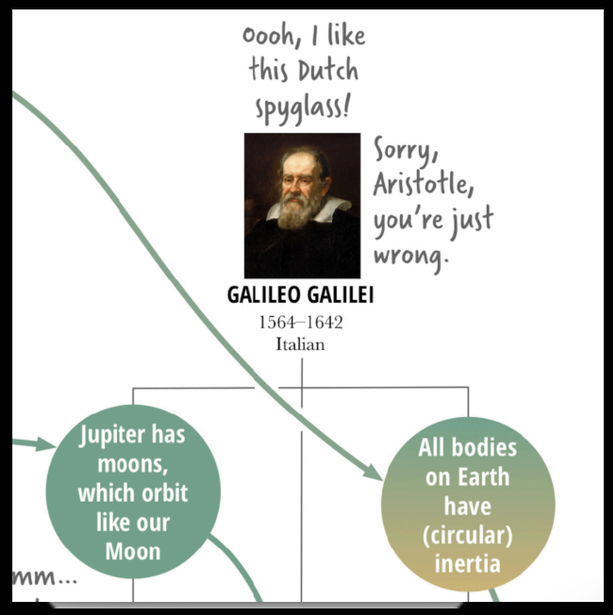

17th Century

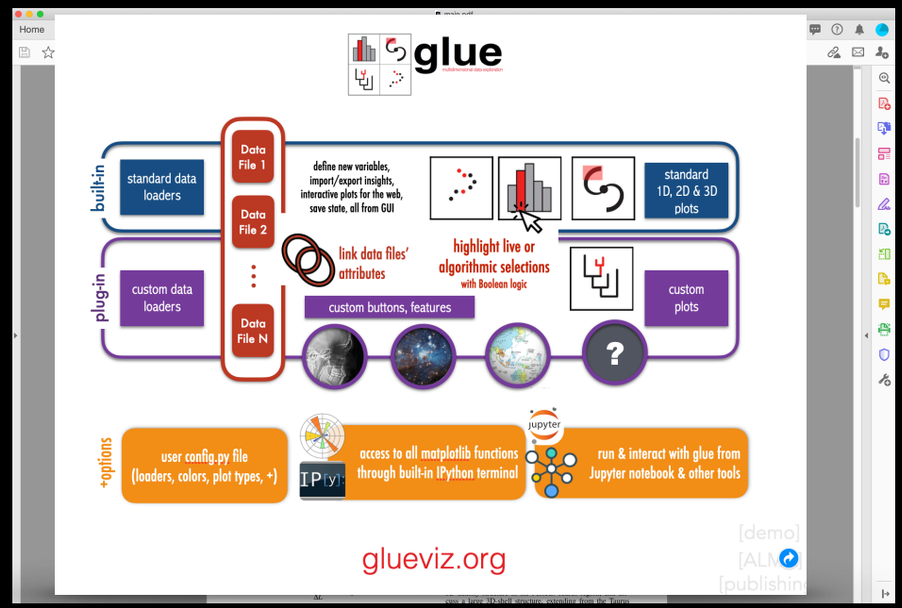

21st Century

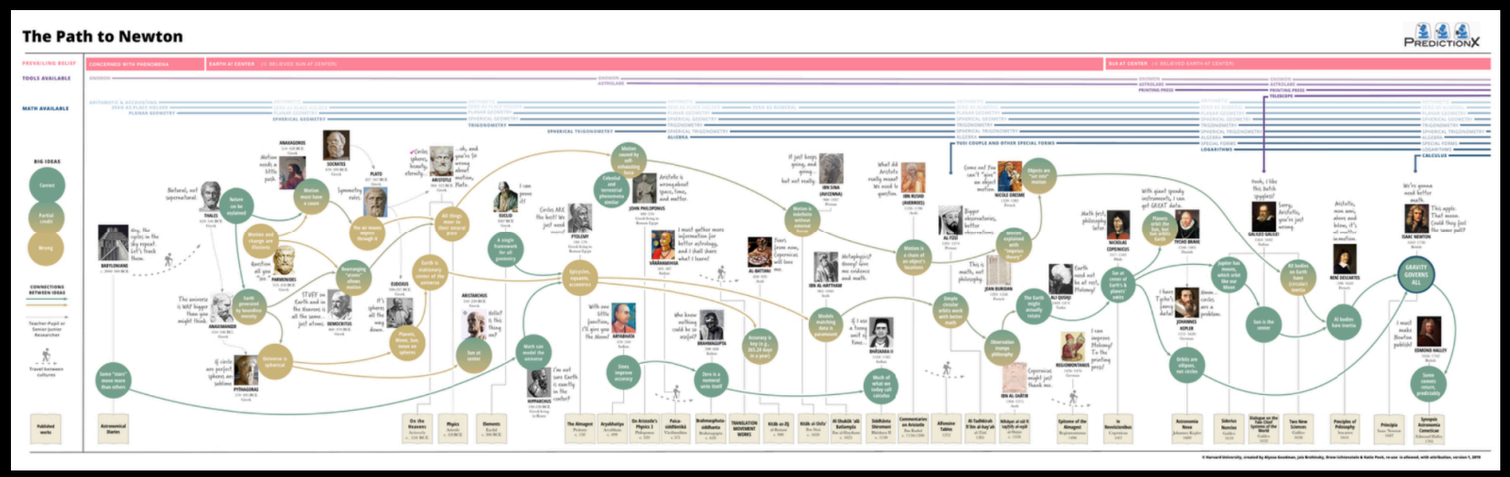

"The Path to Newton"

100 years of Perseus

+2 Challenges...

"case" as a variable...

3D selection

Galileo, Jupiter's Moons, "3D" thinking

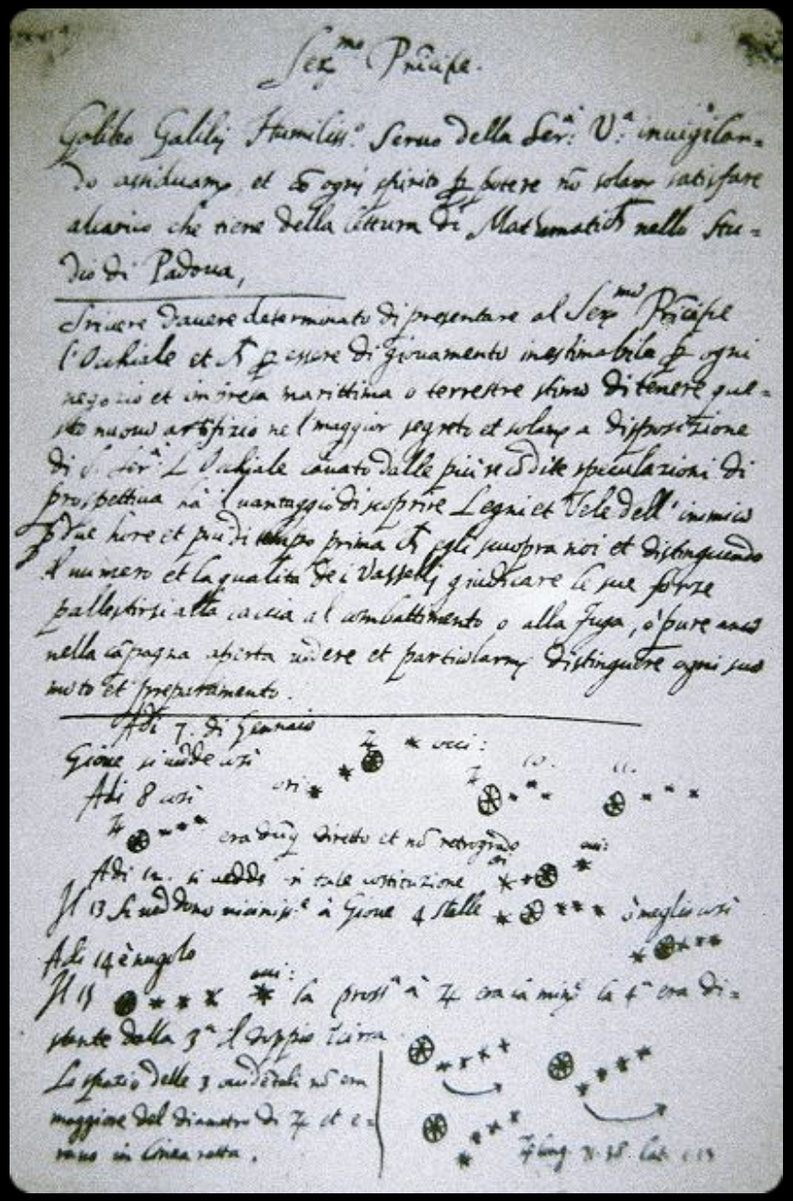

Sen^mo Prencipe.

Galileo Galilei Humilis.^o Servo della Ser.^a V.^a umigliss.^o
Do significare et con ogni spirito di divotione non solam.^te satisfare
all'ufficio che ricerca della Lettura di Mathematica nello Stu-
dio di Padova,

Sendo stato determinato di presentare al Ser.^mo Prencipe
l'Archiale et N.^o essere di giovamento inestimabile a ogni
negotio et impresa marittima o terrestre stimo di tenere qual-
che nuovo artificio nel maggior segreto et solam.^te a disposizione
di V. A. S.^a L'Archiale cavato dalle più sode speculazioni di
prospettiva ha quantaggio di scoprire Legni et Vele dell'inimico
due hore et più di tempo prima che egli scuopra noi et distinguendo
il numero et la qualità de i Vasselli giudicare le sue forze
potendosi alla caccia al combattimento o alla fuga, o pure anco
nella campagna aperta vedere et particolarm.^te distinguere ogni sua
moto et preparamento.

Adì 7. di Genaro
Giove si vedde così
Adì 8 così
Adì 10. si vedde in tale costituzione
Il 13 fu ne Dom.^a mi.^a a Giove 4 stelle disegnate così
Adì 14 è angolo
Il 15 : la prossim.^a a ♃ era di mi.^a la 4.ª era di-
stante dalla 3.ª il doppio di essa
Lo spatio delle 3 vedute no.^n
maggiore del diametro di ♃ et e-
rano in linea retta.

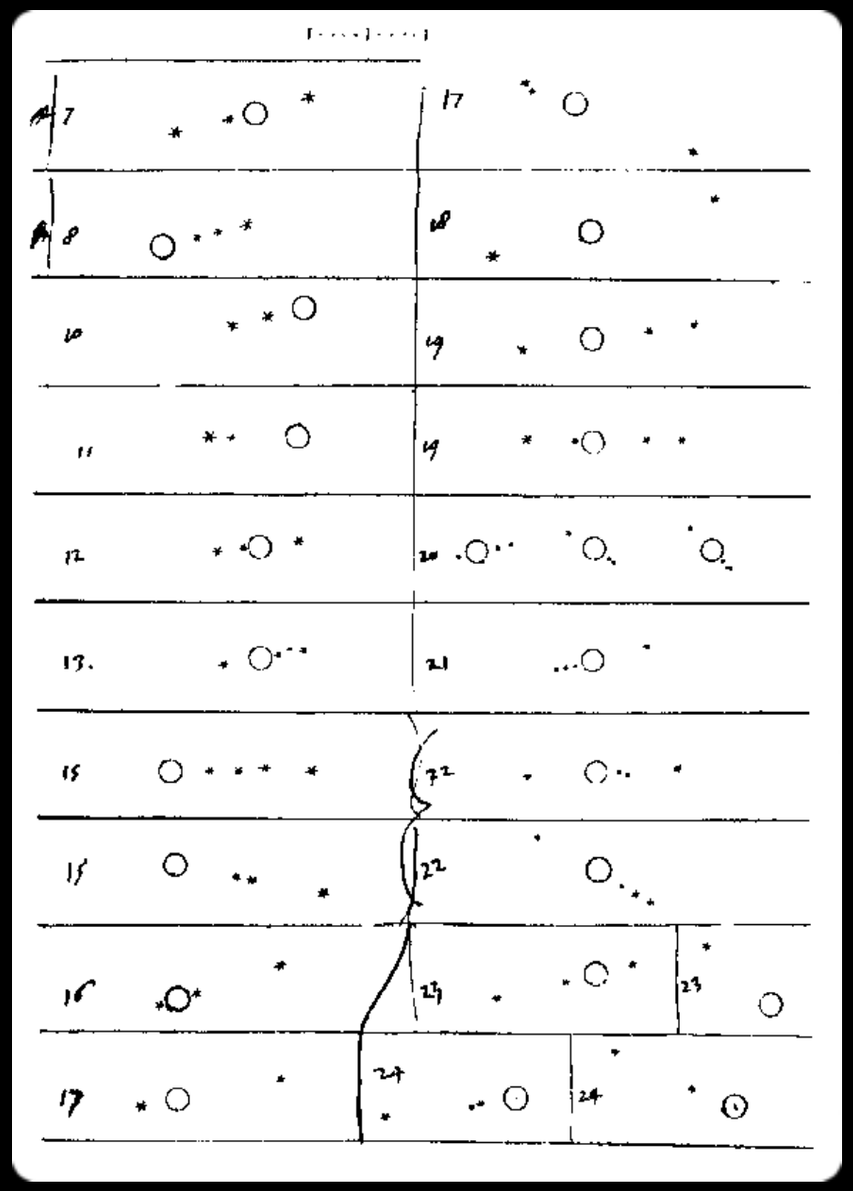

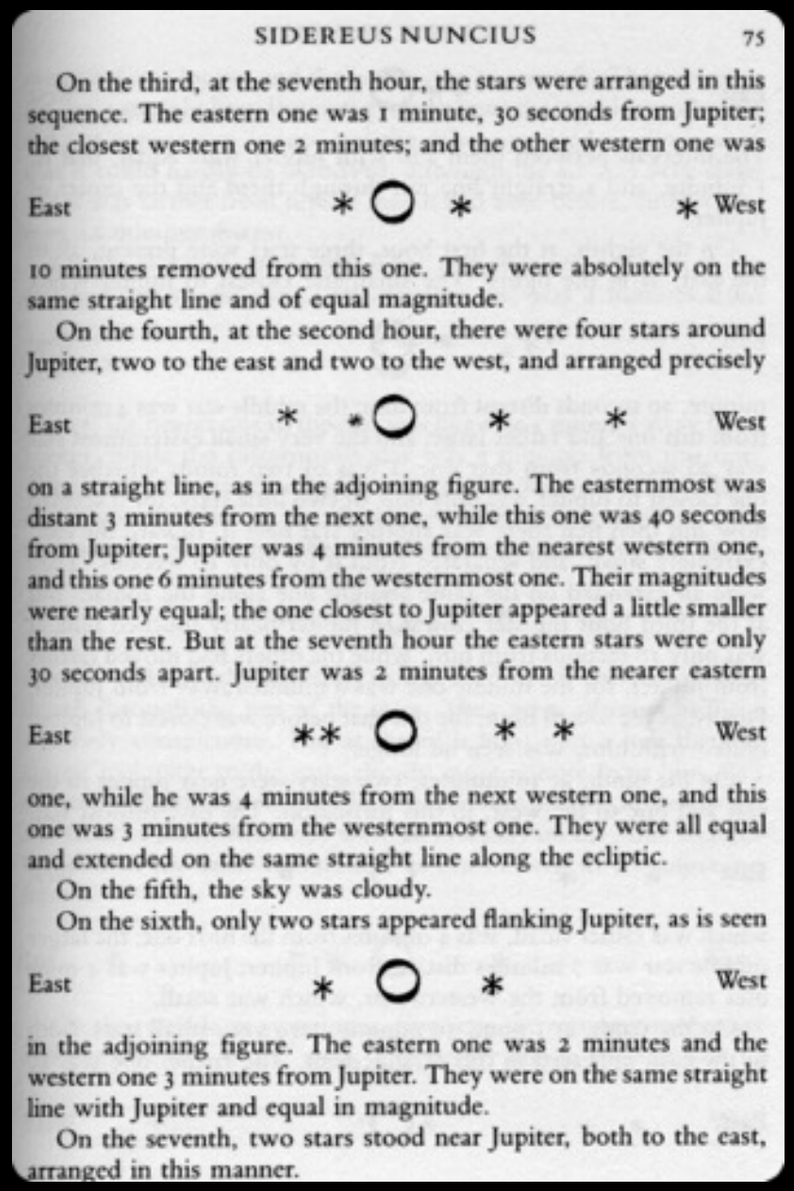

SIDEREUS NUNCIUS 75

On the third, at the seventh hour, the stars were arranged in this sequence. The eastern one was 1 minute, 30 seconds from Jupiter; the closest western one 2 minutes; and the other western one was

East * ○ * * West

10 minutes removed from this one. They were absolutely on the same straight line and of equal magnitude.

On the fourth, at the second hour, there were four stars around Jupiter, two to the east and two to the west, and arranged precisely

East * * ○ * * West

on a straight line, as in the adjoining figure. The easternmost was distant 3 minutes from the next one, while this one was 40 seconds from Jupiter; Jupiter was 4 minutes from the nearest western one, and this one 6 minutes from the westernmost one. Their magnitudes were nearly equal; the one closest to Jupiter appeared a little smaller than the rest. But at the seventh hour the eastern stars were only 30 seconds apart. Jupiter was 2 minutes from the nearer eastern

East ** ○ * * West

one, while he was 4 minutes from the next western one, and this one was 3 minutes from the westernmost one. They were all equal and extended on the same straight line along the ecliptic.

On the fifth, the sky was cloudy.

On the sixth, only two stars appeared flanking Jupiter, as is seen

East * ○ * West

in the adjoining figure. The eastern one was 2 minutes and the western one 3 minutes from Jupiter. They were on the same straight line with Jupiter and equal in magnitude.

On the seventh, two stars stood near Jupiter, both to the east, arranged in this manner.

Notes for & re-productions of Siderius Nuncius

Galileo's 3D thinking, in WorldWide Telescope

January 11, 1610

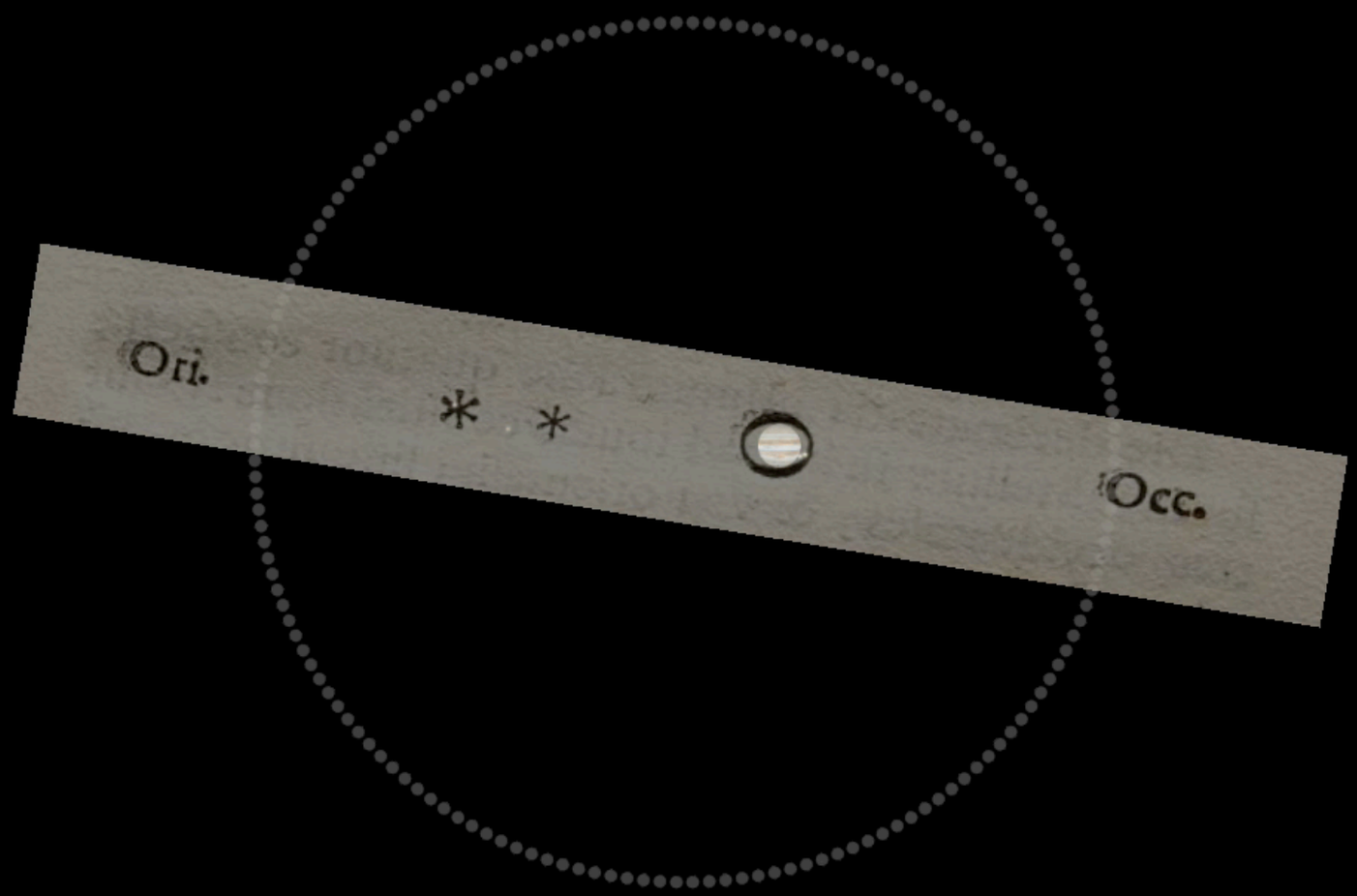

Galileo's New Order, A WorldWide Telescope Tour by Goodman, Wong & Udomprasert 2010
WWT Software Wong (inventor, MS Research), Fay (architect, MS Research), et al., now open source, hosted by AAS
see wwtambassadors.org for more on WWT Outreach

FILTER BY:

Show Sources

ngc 1333

CHOOSE HEATMAP

Object All Stars Galaxies HII regions Nebulae Other

Band Radio Infrared Ultraviolet X-ray

Custom Harvard/All

Year

BACKGROUND LAYER

Optical 2MASS WISE SFD IRIS GLIMPSE H-alpha ROSAT Fermi VLSS

SFD Other

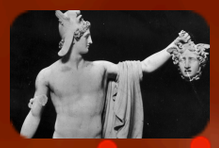

preview/diversion. . .

"Perseus," in WorldWide Telescope (and Aladin, and ESA Sky)

ADS ALL SKY SURVEY

ALADIN

esa Sky

AMERICAN ASTRONOMICAL SOCIETY WORLDWIDE TELESCOPE

(α,δ)=54.39°, 31.54° FOV= 10°

Our Universe is not two-dimensional, but the Sky is.

PERSEUS c. 1918

BLACK & WHITE MONOCHROME IMAGE

Photograph by E. E. Barnard

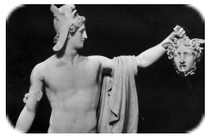

PERSEUS c. 1980s-2006

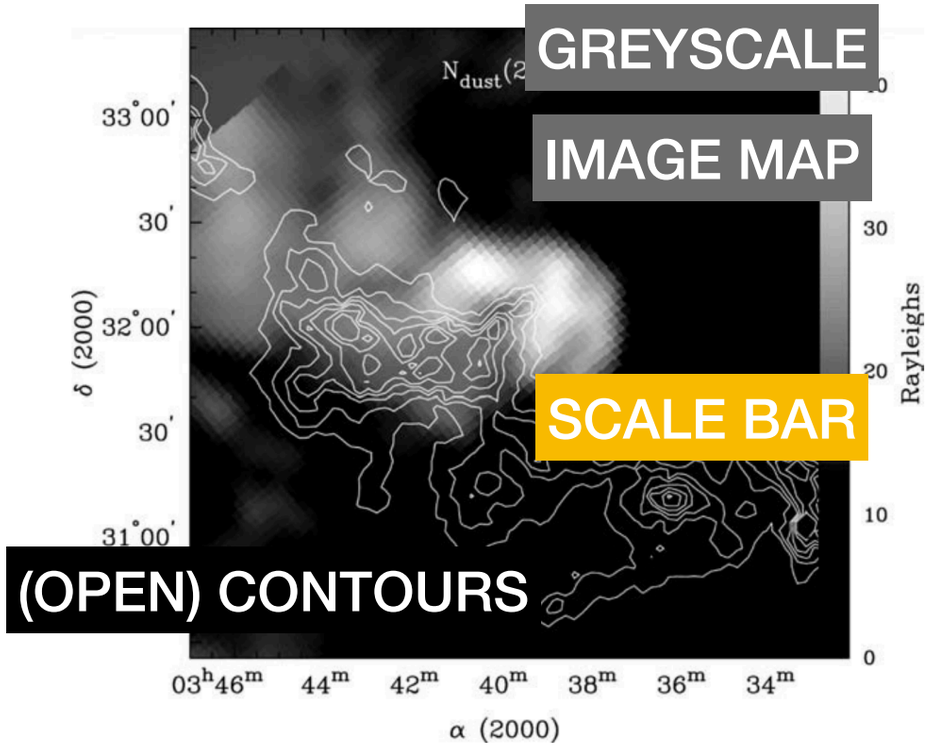

Figure 3. A visual wavelength image of the Perseus molecular cloud. This image was obtained by Adam Block.

Figure 2. An Hα image of G159.6-18.5 from Finkbeiner (2003) overlaid on extinction contours derived from 2MASS/NICER (from Ridge et al. 2006a). The Hα image shows the 1.2° diameter diffuse HII region G159.6-18.5 located behind the Perseus molecular cloud and ionized by the O9.5 / B0.5 star HD 278942.

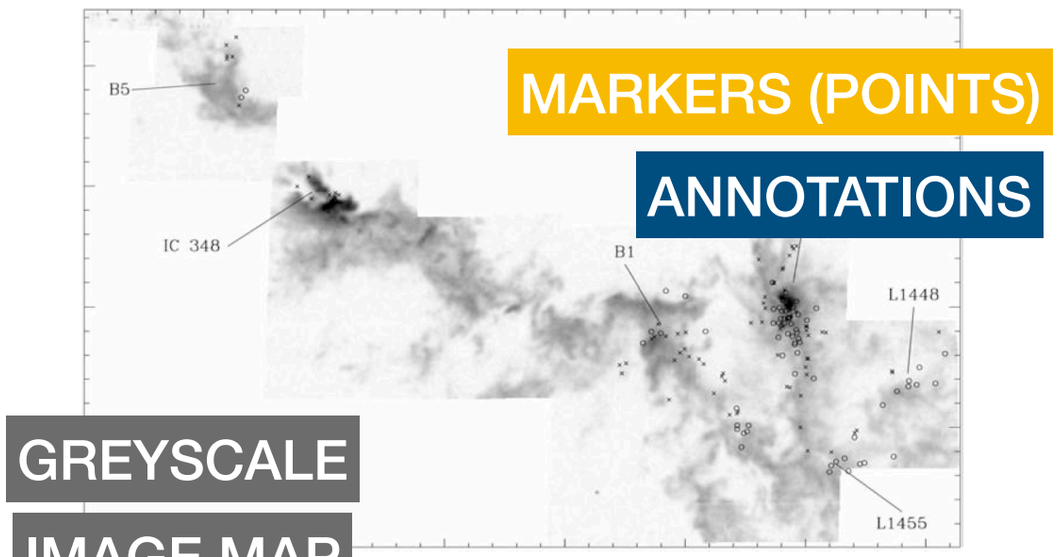

molecular cloud showing the peak antenna temperature of the 110 GHz J = 1 - 0 transition of ^{13}CO. The circles show Herbig-Haro objects discovered prior to the Mosaic CCD survey of Hα and [SII] emission by Walawender et al. (2005a). The crosses show the new objects found in the Mosaic survey.

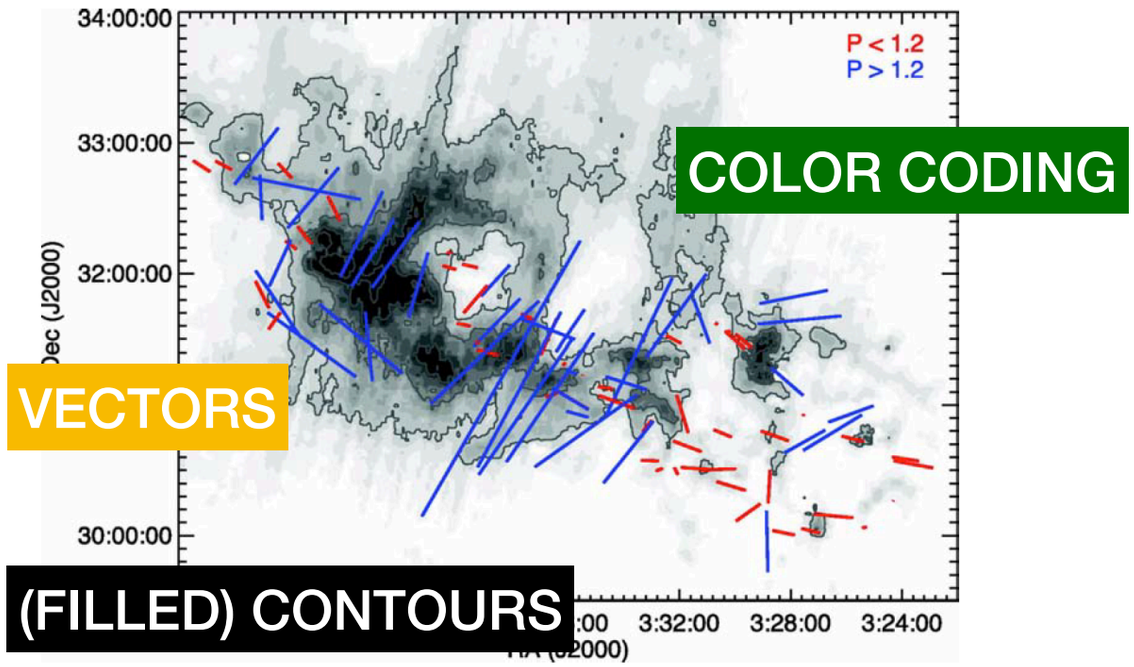

Figure 7. IRAS-derived dust column density overlaid with polarization vectors from Goodman et al. (1990). The polarization vectors shown are parallel to the orientation of the magnetic field in the plane of the sky. Blue vectors have polarization strength P $>$ 1.2% and red vectors have P $<$ 1.2%. The stronger polarization may trace warm dust associated with the IRAS dust (courtesy of the COMPLETE team).

All figures reproduced from in Bally et al. 2008, which cites original sources

PERSEUS 2007-2010

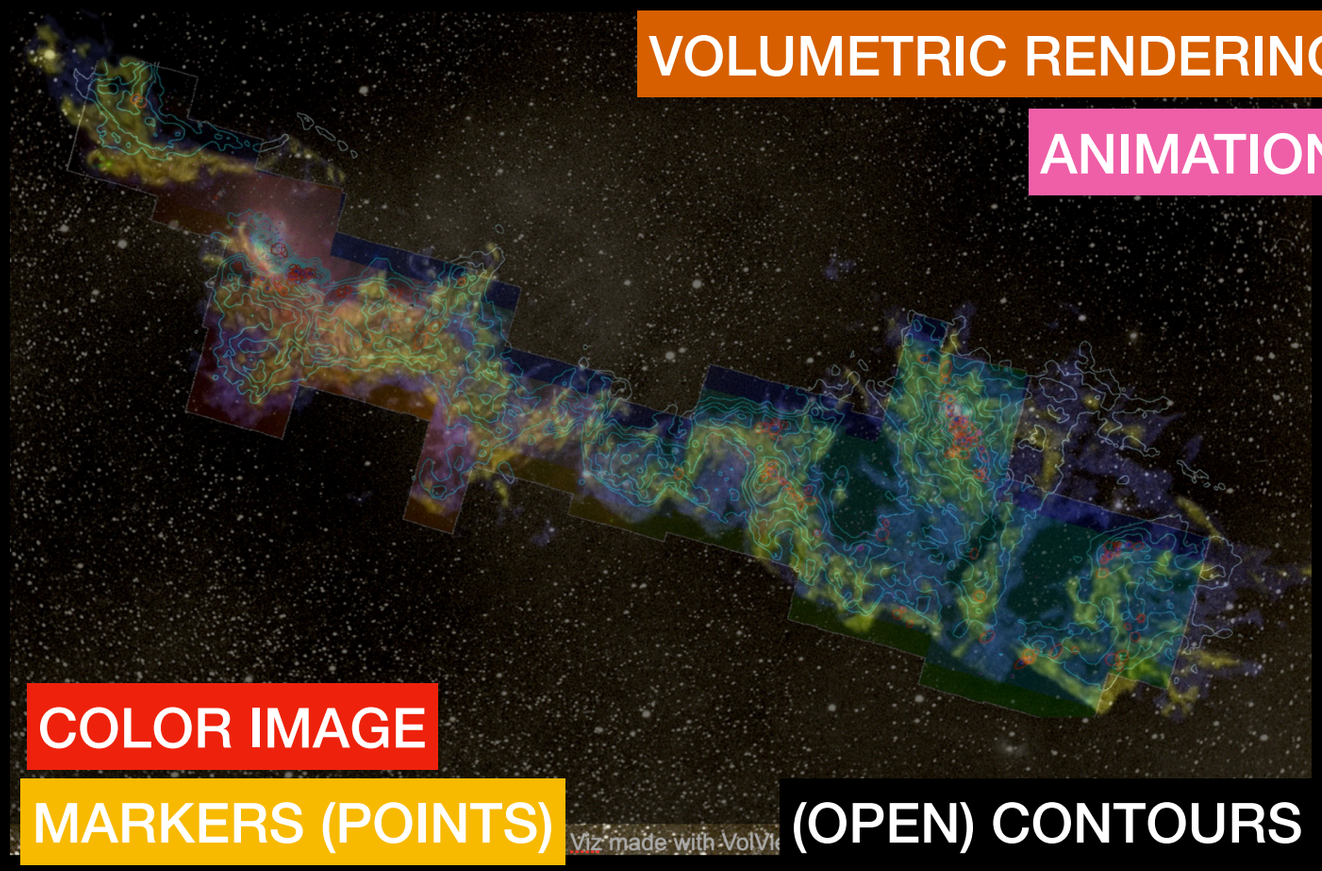

VOLUMETRIC RENDERING

ANIMATION

COLOR IMAGE

MARKERS (POINTS)

(OPEN) CONTOURS

Viz made with VolVi

AstronomicalMedicine@IIC

COMPLETE

INTERACTIVITY

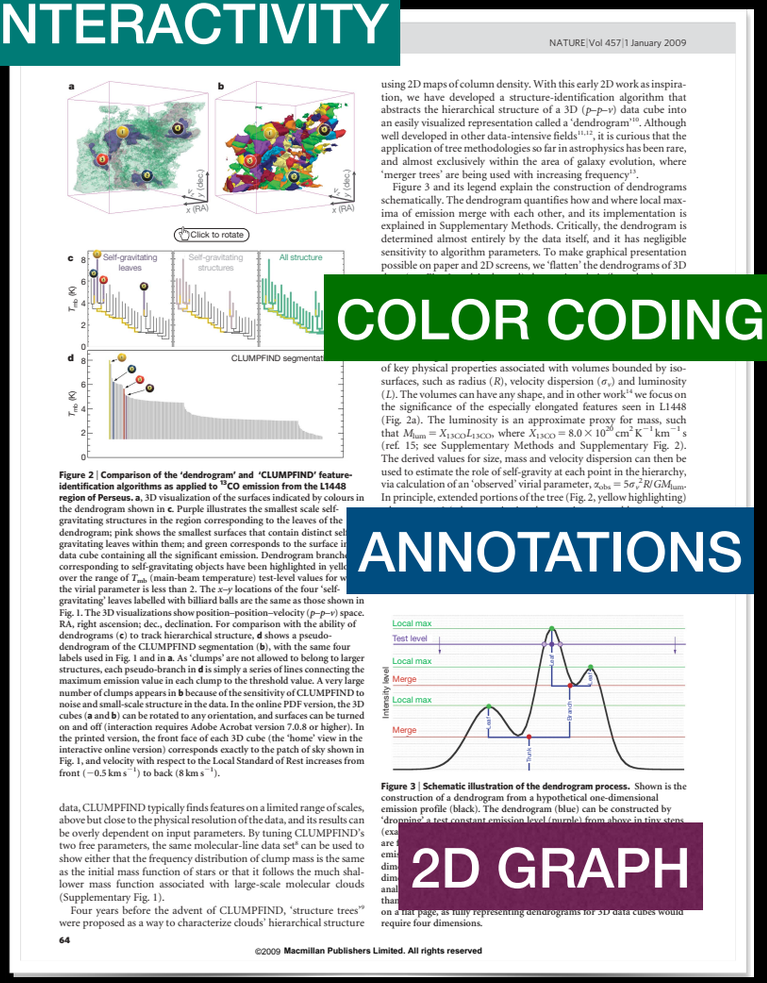

NATURE|Vol 457|1 January 2009

Click to rotate

Self-gravitating leaves

Self-gravitating structures

All structure

CLUMPFIND segmentation

Figure 2 | Comparison of the 'dendrogram' and 'CLUMPFIND' feature-identification algorithms as applied to ^{13}CO emission from the L1448 region of Perseus. a, 3D visualization of the surfaces indicated by colours in the dendrogram shown in c. Purple illustrates the smallest scale self-gravitating structures in the region corresponding to the leaves of the dendrogram; pink shows the smallest surfaces that contain distinct self-gravitating leaves within them; and green corresponds to the surface in data cube containing all the significant emission. Dendrogram branches corresponding to self-gravitating objects have been highlighted in yellow over the range of T_{mb} (main-beam temperature) test-level values for which the virial parameter is less than 2. The x–y locations of the four 'self-gravitating' leaves labelled with billiard balls are the same as those shown in Fig. 1. The 3D visualizations show position–position–velocity (p–p–v) space. RA, right ascension; dec., declination. For comparison with the ability of dendrograms (c) to track hierarchical structure, d shows a pseudo-dendrogram of the CLUMPFIND segmentation (b), with the same four labels used in Fig. 1 and in a. As 'clumps' are not allowed to belong to larger structures, each pseudo-branch in d is simply a series of lines connecting the maximum emission value in each clump to the threshold value. A very large number of clumps appears in b because of the sensitivity of CLUMPFIND to noise and small-scale structure in the data. In the online PDF version, the 3D cubes (a and b) can be rotated to any orientation, and surfaces can be turned on and off (interaction requires Adobe Acrobat version 7.0.8 or higher). In the printed version, the front face of each 3D cube (the 'home' view in the interactive online version) corresponds exactly to the patch of sky shown in Fig. 1, and velocity with respect to the Local Standard of Rest increases from front (−0.5 km s^{-1}) to back (8 km s^{-1}).

data, CLUMPFIND typically finds features on a limited range of scales, above but close to the physical resolution of the data, and its results can be overly dependent on input parameters. By tuning CLUMPFIND's two free parameters, the same molecular-line data set[6] can be used to show either that the frequency distribution of clump mass is the same as the initial mass function of stars or that it follows the much shallower mass function associated with large-scale molecular clouds (Supplementary Fig. 1).

Four years before the advent of CLUMPFIND, 'structure trees'[29] were proposed as a way to characterize clouds' hierarchical structure

64

©2009 Macmillan Publishers Limited. All rights reserved

using 2D maps of column density. With this early 2D work as inspiration, we have developed a structure-identification algorithm that abstracts the hierarchical structure of a 3D (p–p–v) data cube into an easily visualized representation called a 'dendrogram'[10]. Although well developed in other data-intensive fields[11,12], it is curious that the application of tree methodologies so far in astrophysics has been rare, and almost exclusively within the area of galaxy evolution, where 'merger trees' are being used with increasing frequency[13].

Figure 3 and its legend explain the construction of dendrograms schematically. The dendrogram quantifies how and where local maxima of emission merge with each other, and its implementation is explained in Supplementary Methods. Critically, the dendrogram is determined almost entirely by the data itself, and it has negligible sensitivity to algorithm parameters. To make graphical presentation possible on paper and 2D screens, we 'flatten' the dendrograms of 3D

of key physical properties associated with volumes bounded by isosurfaces, such as radius (R), velocity dispersion (σ_v) and luminosity (L). The volumes can have any shape, and in other work[14] we focus on the significance of the especially elongated features seen in L1448 (Fig. 2a). The luminosity is an approximate proxy for mass, such that $M_{lum} = X_{13CO} L_{13CO}$, where $X_{13CO} = 8.0 \times 10^{20}$ cm^{-2} K^{-1} km^{-1} s (ref. 15; see Supplementary Methods and Supplementary Fig. 2). The derived values for size, mass and velocity dispersion can then be used to estimate the role of self-gravity at each point in the hierarchy, via calculation of an 'observed' virial parameter, $\alpha_{obs} = 5\sigma_v^2 R/GM_{lum}$. In principle, extended portions of the tree (Fig. 2, yellow highlighting)

COLOR CODING

ANNOTATIONS

Local max

Test level

Local max

Merge

Local max

Merge

Intensity level

1 and 2

3 and 4

Figure 3 | Schematic illustration of the dendrogram process. Shown is the construction of a dendrogram from a hypothetical one-dimensional emission profile (black). The dendrogram (blue) can be constructed by 'dropping' a test constant emission level (purple) from above in tiny steps (exa... are ... emi... dim... dim... anal... that...

on a flat page, as fully representing dendrograms for 3D data cubes would require four dimensions.

2D GRAPH

"Astronomical Medicine"

2006-2010

"3D PDF"

2009

Largely thanks to work of the "Astronomical Medicine" project at the Harvard IIC (with Borkin, Halle, Kauffmann et al.)

Diverse High-Dimensional Data

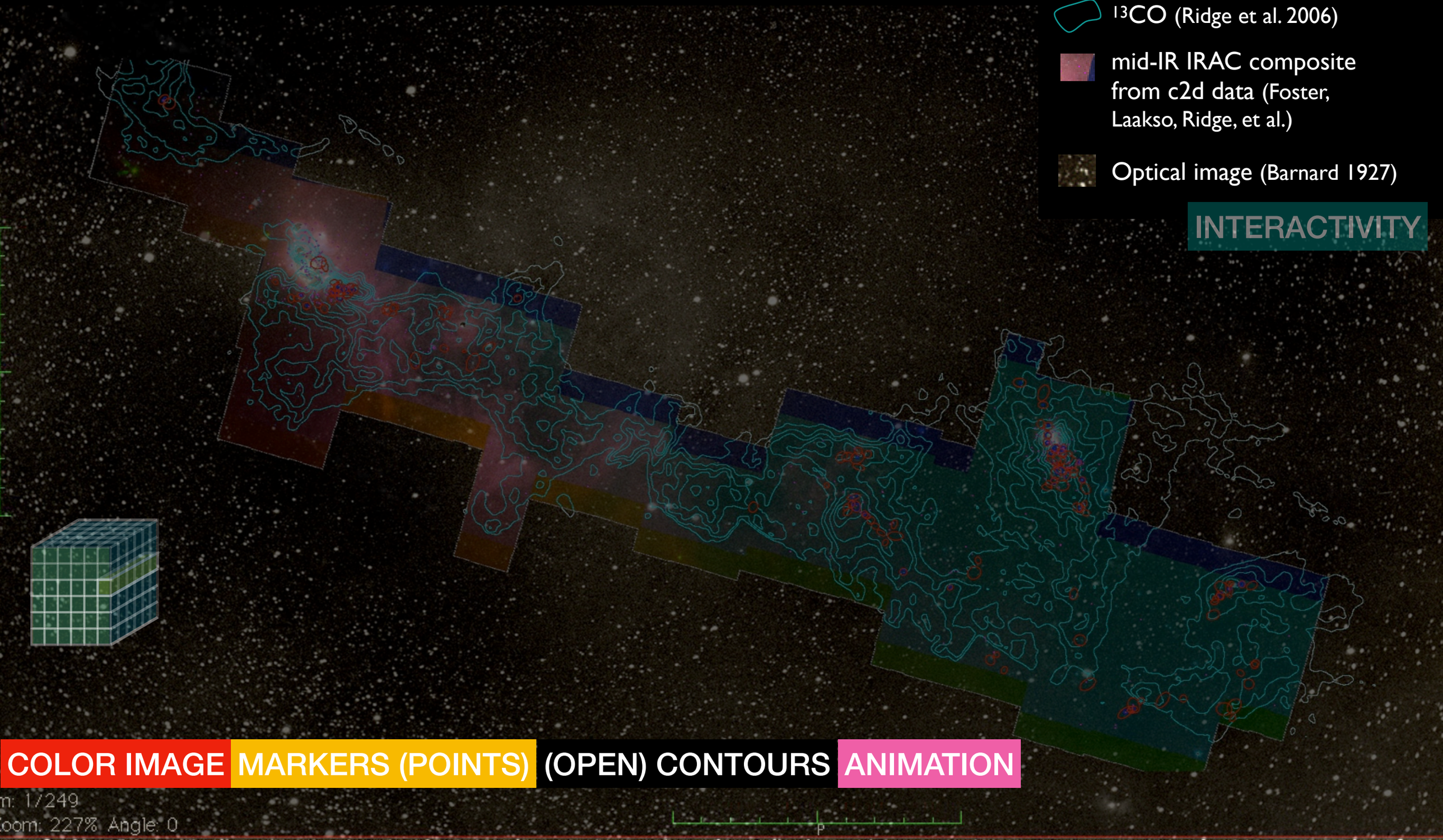

INTERACTIVITY

COLOR IMAGE | MARKERS (POINTS) | (OPEN) CONTOURS | ANIMATION | VOLUMETRIC RENDERING

3D Viz made with VolView

AstronomicalMedicine@IIG

COMPLETE

PERSEUS 2007-2010

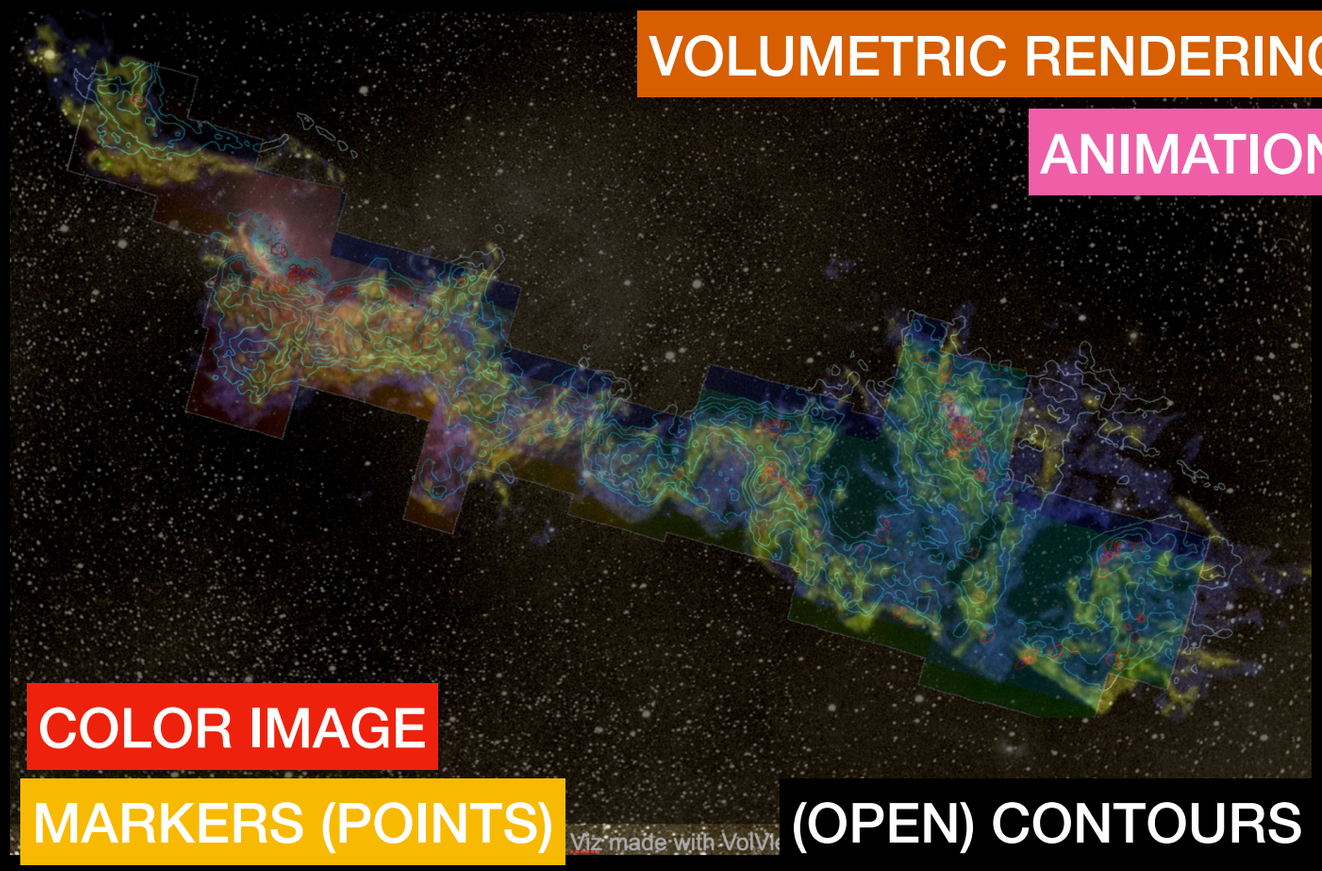

VOLUMETRIC RENDERING

ANIMATION

COLOR IMAGE

MARKERS (POINTS)

(OPEN) CONTOURS

Viz made with VolVi

AstronomicalMedicine@IIC

COMPLETE

INTERACTIVITY

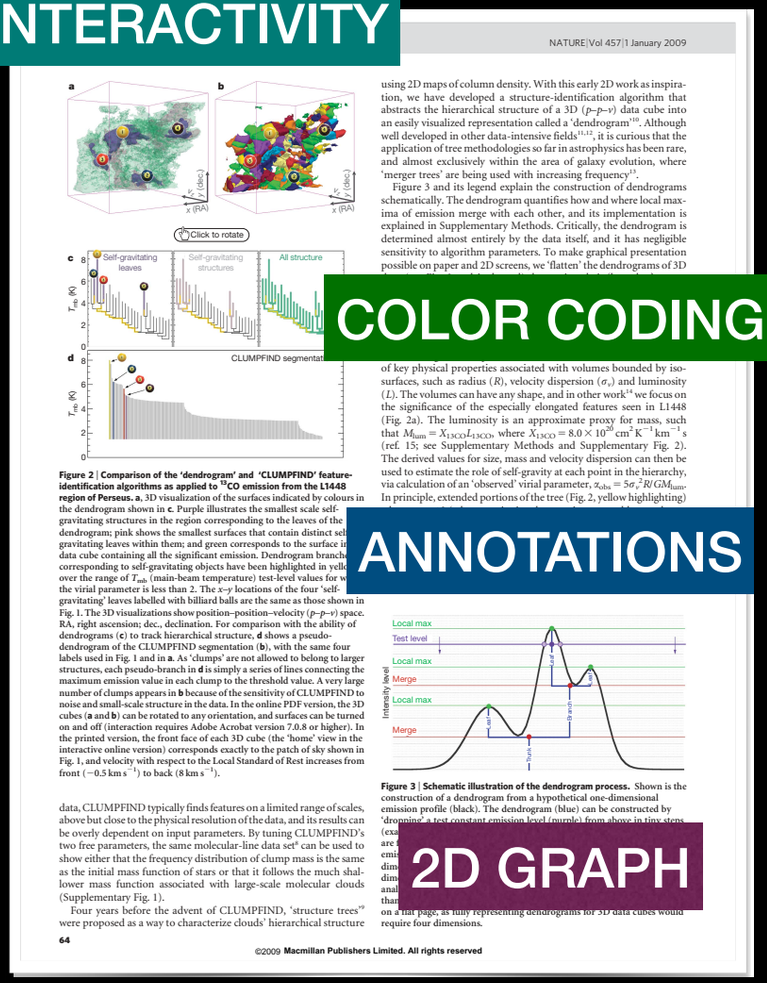

NATURE|Vol 457|1 January 2009

Click to rotate

Self-gravitating leaves

Self-gravitating structures

All structure

CLUMPFIND segmentation

Figure 2 | Comparison of the 'dendrogram' and 'CLUMPFIND' feature-identification algorithms as applied to ^{13}CO emission from the L1448 region of Perseus. a, 3D visualization of the surfaces indicated by colours in the dendrogram shown in c. Purple illustrates the smallest scale self-gravitating structures in the region corresponding to the leaves of the dendrogram; pink shows the smallest surfaces that contain distinct self-gravitating leaves within them; and green corresponds to the surface in data cube containing all the significant emission. Dendrogram branches corresponding to self-gravitating objects have been highlighted in yellow over the range of T_{mb} (main-beam temperature) test-level values for which the virial parameter is less than 2. The x–y locations of the four 'self-gravitating' leaves labelled with billiard balls are the same as those shown in Fig. 1. The 3D visualizations show position–position–velocity (p–p–v) space. RA, right ascension; dec., declination. For comparison with the ability of dendrograms (c) to track hierarchical structure, d shows a pseudo-dendrogram of the CLUMPFIND segmentation (b), with the same four labels used in Fig. 1 and in a. As 'clumps' are not allowed to belong to larger structures, each pseudo-branch in d is simply a series of lines connecting the maximum emission value in each clump to the threshold value. A very large number of clumps appears in b because of the sensitivity of CLUMPFIND to noise and small-scale structure in the data. In the online PDF version, the 3D cubes (a and b) can be rotated to any orientation, and surfaces can be turned on and off (interaction requires Adobe Acrobat version 7.0.8 or higher). In the printed version, the front face of each 3D cube (the 'home' view in the interactive online version) corresponds exactly to the patch of sky shown in Fig. 1, and velocity with respect to the Local Standard of Rest increases from front (−0.5 km s^{-1}) to back (8 km s^{-1}).

data, CLUMPFIND typically finds features on a limited range of scales, above but close to the physical resolution of the data, and its results can be overly dependent on input parameters. By tuning CLUMPFIND's two free parameters, the same molecular-line data set[6] can be used to show either that the frequency distribution of clump mass is the same as the initial mass function of stars or that it follows the much shallower mass function associated with large-scale molecular clouds (Supplementary Fig. 1).

Four years before the advent of CLUMPFIND, 'structure trees'[29] were proposed as a way to characterize clouds' hierarchical structure

64

©2009 Macmillan Publishers Limited. All rights reserved

using 2D maps of column density. With this early 2D work as inspiration, we have developed a structure-identification algorithm that abstracts the hierarchical structure of a 3D (p–p–v) data cube into an easily visualized representation called a 'dendrogram'[10]. Although well developed in other data-intensive fields[11,12], it is curious that the application of tree methodologies so far in astrophysics has been rare, and almost exclusively within the area of galaxy evolution, where 'merger trees' are being used with increasing frequency[13].

Figure 3 and its legend explain the construction of dendrograms schematically. The dendrogram quantifies how and where local maxima of emission merge with each other, and its implementation is explained in Supplementary Methods. Critically, the dendrogram is determined almost entirely by the data itself, and it has negligible sensitivity to algorithm parameters. To make graphical presentation possible on paper and 2D screens, we 'flatten' the dendrograms of 3D

of key physical properties associated with volumes bounded by isosurfaces, such as radius (R), velocity dispersion (σ_v) and luminosity (L). The volumes can have any shape, and in other work[14] we focus on the significance of the especially elongated features seen in L1448 (Fig. 2a). The luminosity is an approximate proxy for mass, such that $M_{lum} = X_{13CO} L_{13CO}$, where $X_{13CO} = 8.0 \times 10^{20}$ cm^{-2} K^{-1} km^{-1} s (ref. 15; see Supplementary Methods and Supplementary Fig. 2). The derived values for size, mass and velocity dispersion can then be used to estimate the role of self-gravity at each point in the hierarchy, via calculation of an 'observed' virial parameter, $\alpha_{obs} = 5\sigma_v^2 R/GM_{lum}$. In principle, extended portions of the tree (Fig. 2, yellow highlighting)

COLOR CODING

ANNOTATIONS

Local max

Test level

Local max

Merge

Local max

Merge

Intensity level

1 and 2

3 and 4

Figure 3 | Schematic illustration of the dendrogram process. Shown is the construction of a dendrogram from a hypothetical one-dimensional emission profile (black). The dendrogram (blue) can be constructed by 'dropping' a test constant emission level (purple) from above in tiny steps (exa... are ... emi... dim... dim... anal... that...

on a flat page, as fully representing dendrograms for 3D data cubes would require four dimensions.

2D GRAPH

"Astronomical Medicine"

2006-2010

"3D PDF"

2009

Largely thanks to work of the "Astronomical Medicine" project at the Harvard IIC (with Borkin, Halle, Kauffmann et al.)

2009

3D PDF

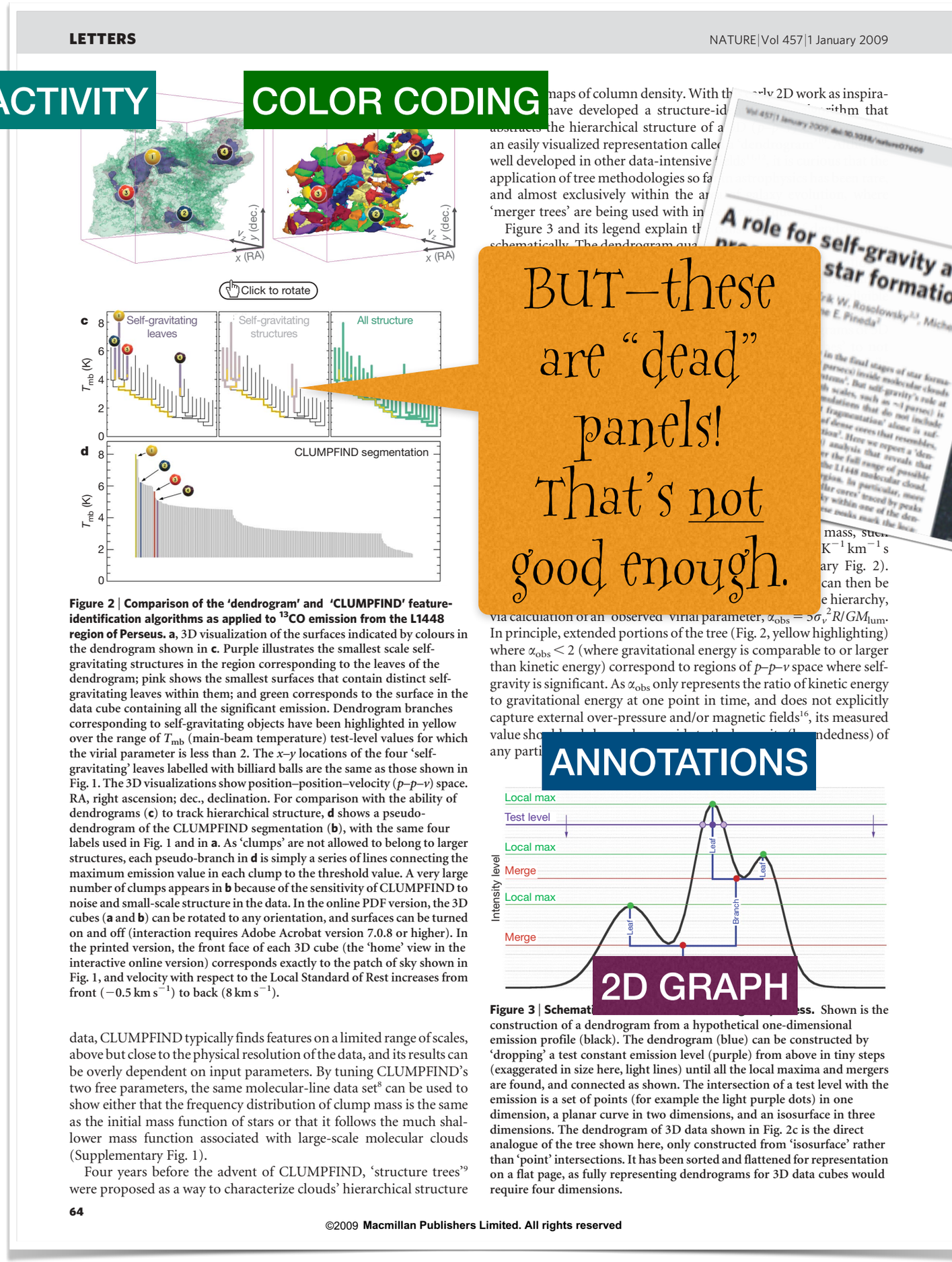

Figure 2 | Comparison of the 'dendrogram' and 'CLUMPFIND' feature-identification algorithms as applied to ^{13}CO emission from the L1448 region of Perseus. a, 3D visualization of the surfaces indicated by colours in the dendrogram shown in **c**. Purple illustrates the smallest scale self-gravitating structures in the region corresponding to the leaves of the dendrogram; pink shows the smallest surfaces that contain distinct self-gravitating leaves within them; and green corresponds to the surface in the data cube containing all the significant emission. Dendrogram branches corresponding to self-gravitating objects have been highlighted in yellow over the range of T_{mb} (main-beam temperature) test-level values for which the virial parameter is less than 2. The x–y locations of the four 'self-gravitating' leaves labelled with billiard balls are the same as those shown in Fig. 1. The 3D visualizations show position–position–velocity (p–p–v) space. RA, right ascension; dec., declination. For comparison with the ability of dendrograms (**c**) to track hierarchical structure, **d** shows a pseudo-dendrogram of the CLUMPFIND segmentation (**b**), with the same four labels used in Fig. 1 and in **a**. As 'clumps' are not allowed to belong to larger structures, each pseudo-branch in **d** is simply a series of lines connecting the maximum emission value in each clump to the threshold value. A very large number of clumps appears in **b** because of the sensitivity of CLUMPFIND to noise and small-scale structure in the data. In the online PDF version, the 3D cubes (**a** and **b**) can be rotated to any orientation, and surfaces can be turned on and off (interaction requires Adobe Acrobat version 7.0.8 or higher). In the printed version, the front face of each 3D cube (the 'home' view in the interactive online version) corresponds exactly to the patch of sky shown in Fig. 1, and velocity with respect to the Local Standard of Rest increases from front (-0.5 km s^{-1}) to back (8 km s^{-1}).

data, CLUMPFIND typically finds features on a limited range of scales, above but close to the physical resolution of the data, and its results can be overly dependent on input parameters. By tuning CLUMPFIND's two free parameters, the same molecular-line data set[8] can be used to show either that the frequency distribution of clump mass is the same as the initial mass function of stars or that it follows the much shallower mass function associated with large-scale molecular clouds (Supplementary Fig. 1).

Four years before the advent of CLUMPFIND, 'structure trees'[9] were proposed as a way to characterize clouds' hierarchical structure

maps of column density. With th... 2D work as inspira-
have developed a structure-id... rithm that
abstracts the hierarchical structure of a...
an easily visualized representation calle...
well developed in other data-intensive...
application of tree methodologies so fa...
and almost exclusively within the ar...
'merger trees' are being used with in...
Figure 3 and its legend explain th...
schematically. The dendrogram qua...

BUT—these are "dead" panels! That's not good enough.

mass, such...
K^{-1} km^{-1} s
ary Fig. 2).
can then be
e hierarchy,
via calculation of an 'observed' virial parameter, $\alpha_{obs} = 5\sigma_v^2 R/GM_{lum}$.
In principle, extended portions of the tree (Fig. 2, yellow highlighting) where $\alpha_{obs} < 2$ (where gravitational energy is comparable to or larger than kinetic energy) correspond to regions of p–p–v space where self-gravity is significant. As α_{obs} only represents the ratio of kinetic energy to gravitational energy at one point in time, and does not explicitly capture external over-pressure and/or magnetic fields[16], its measured value sho... ndedness) of any parti...

ANNOTATIONS

Local max
Test level
Local max
Merge
Local max
Merge
Intensity level
Leaf
Branch
Leaf
Leaf

2D GRAPH

Figure 3 | Schemati... ss. Shown is the construction of a dendrogram from a hypothetical one-dimensional emission profile (black). The dendrogram (blue) can be constructed by 'dropping' a test constant emission level (purple) from above in tiny steps (exaggerated in size here, light lines) until all the local maxima and mergers are found, and connected as shown. The intersection of a test level with the emission is a set of points (for example the light purple dots) in one dimension, a planar curve in two dimensions, and an isosurface in three dimensions. The dendrogram of 3D data shown in Fig. 2c is the direct analogue of the tree shown here, only constructed from 'isosurface' rather than 'point' intersections. It has been sorted and flattened for representation on a flat page, as fully representing dendrograms for 3D data cubes would require four dimensions.

64

©2009 Macmillan Publishers Limited. All rights reserved

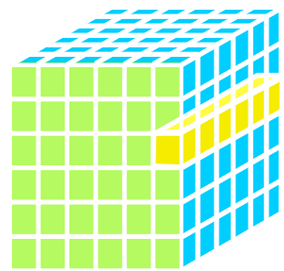

Goodman et al. 2009, Nature,
cf: Fluke et al. 2009

"3D PDF" (Nature, 2009)

Vol 457|1 January 2009|doi:10.1038/nature07609

nature

LETTERS

A role for self-gravity at multiple length scales in the process of star formation

Alyssa A. Goodman[1,2], Erik W. Rosolowsky[2,3], Michelle A. Borkin[1]†, Jonathan B. Foster[2], Michael Halle[1,4], Jens Kauffmann[1,2] & Jaime E. Pineda[2]

Self-gravity plays a decisive role in the final stages of star formation, where dense cores (size ~0.1 parsecs) inside molecular clouds collapse to form star-plus-disk systems[1]. But self-gravity's role at earlier times (and on larger length scales, such as ~1 parsec) is unclear; some molecular cloud simulations that do not include self-gravity suggest that 'turbulent fragmentation' alone is sufficient to create a mass distribution of dense cores that resembles, and sets, the stellar initial mass function[2]. Here we report a 'dendrogram' (hierarchical tree-diagram) analysis that reveals that self-gravity plays a significant role over the full range of possible scales traced by ^{13}CO observations in the L1448 molecular cloud, but not everywhere in the observed region. In particular, more than 90 per cent of the compact 'pre-stellar cores' traced by peaks of dust emission[3] are projected on the sky within one of the dendrogram's self-gravitating 'leaves'. As these peaks mark the locations of already-forming stars, or of those probably about to form, a self-gravitating cocoon seems a critical condition for their exist-

overlapping features as an option, significant emission found between prominent clumps is typically either appended to the nearest clump or turned into a small, usually 'pathological', feature needed to encompass all the emission being modelled. When applied to molecular-line

Linked Views of High-dimensional Data

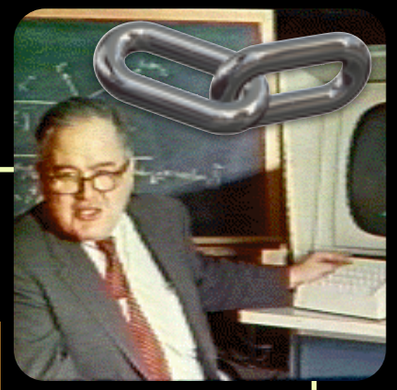

John Tukey

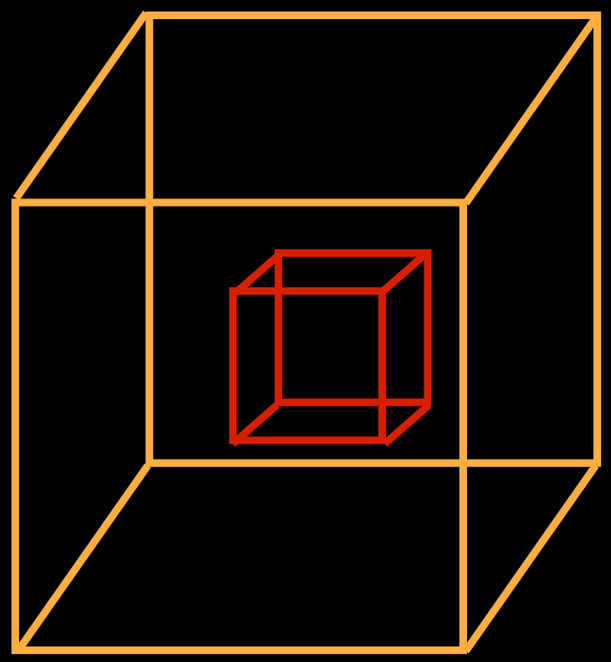

3D

2D

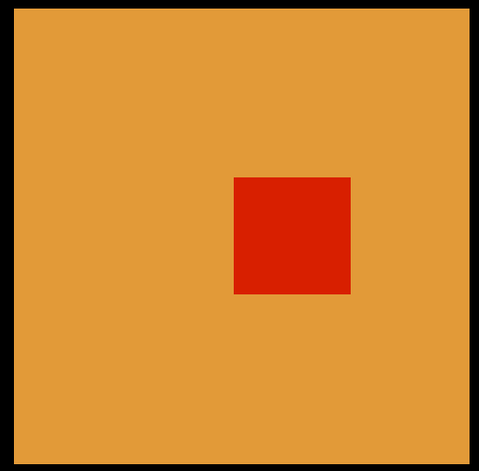

glue

Statistics

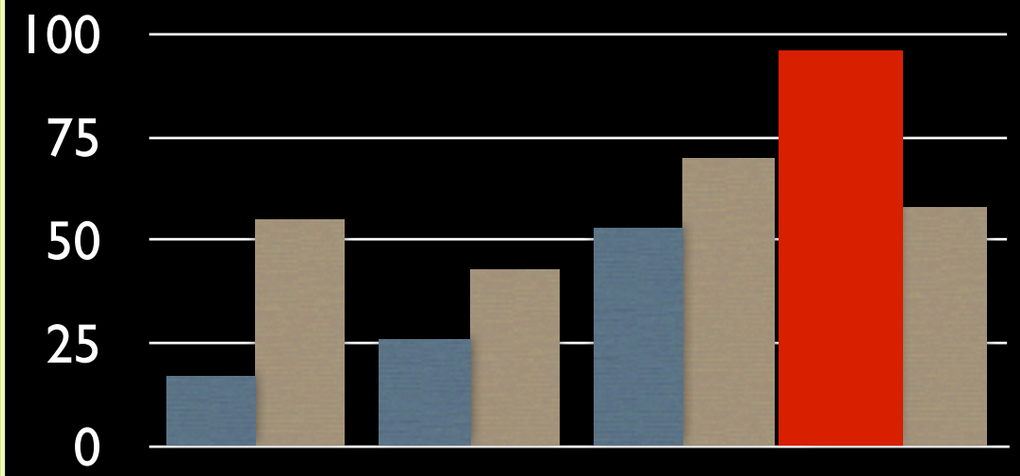

Data Abstraction

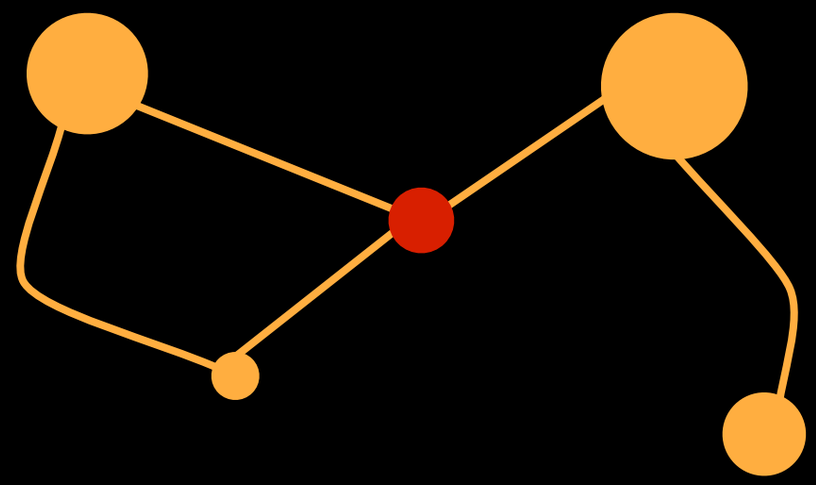

figure, by M. Borkin, reproduced from Goodman 2012, "Principles of High-Dimensional Data Visualization in Astronomy"

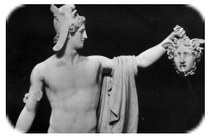

PERSEUS 2011-2020

glue
multidimensional data exploration

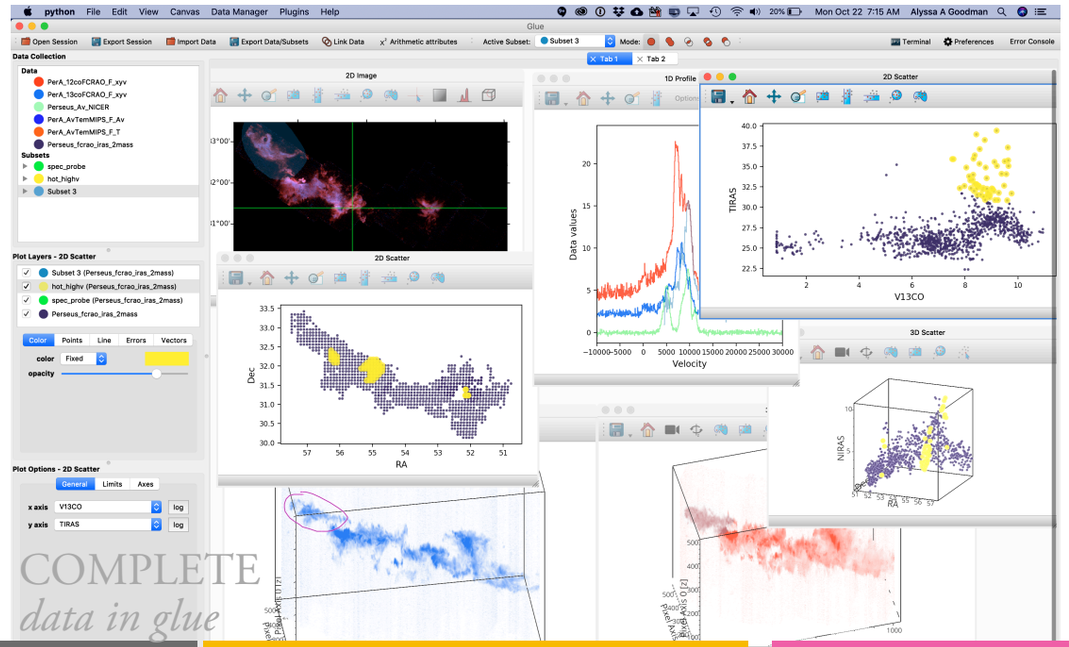

COMPLETE
data in glue

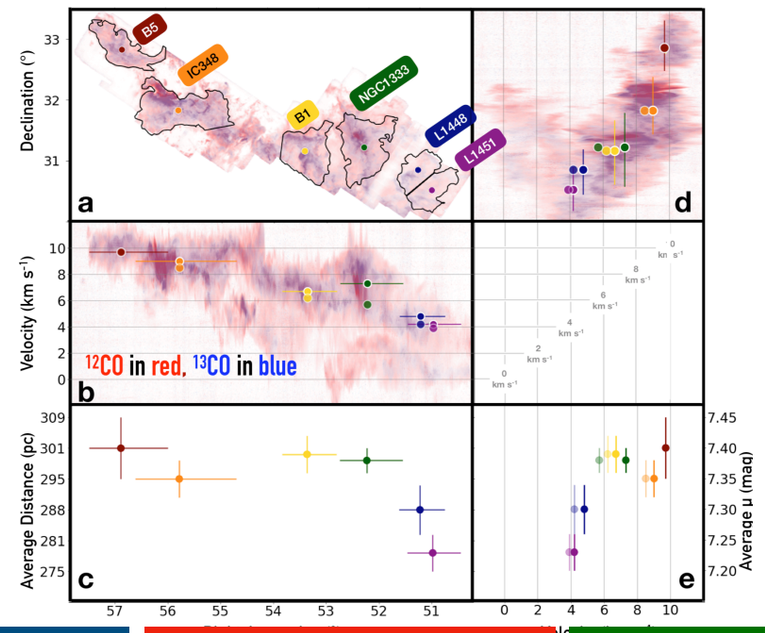

Zucker et al. 2018

GREYSCALE | MARKERS (POINTS) | ANIMATION | ANNOTATIONS | COLOR IMAGE | COLOR CODING

SCALE BAR | VOLUMETRIC RENDERING | INTERACTIVITY | VECTORS | CONTOURS | IMAGE MAP

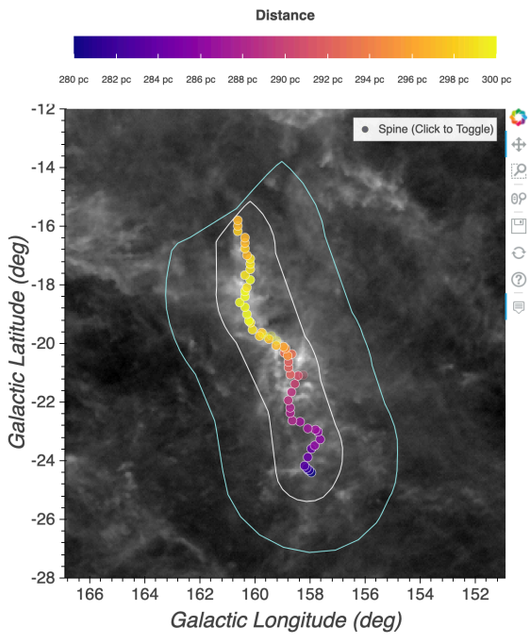

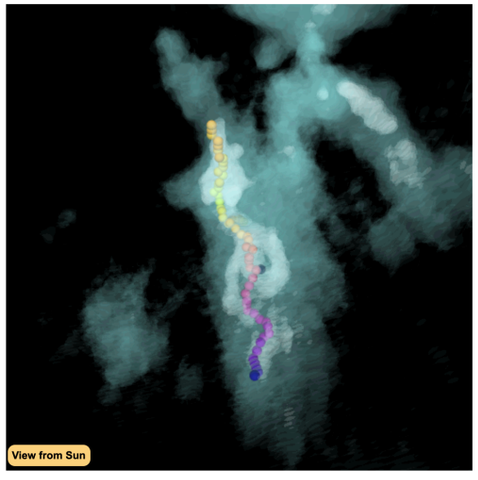

Zucker et al. 2020

AUGMENTED REALITY(!)

Bialy et al. 2020

Many thanks to Catherine Zucker, Tom Robitaille, Chris Beaumont, Michelle Borkin, Maarten Breddels, Penny Qian, et al.

Linked Views of High-dimensional Data (in Python)

glue *(and glupyter!)*

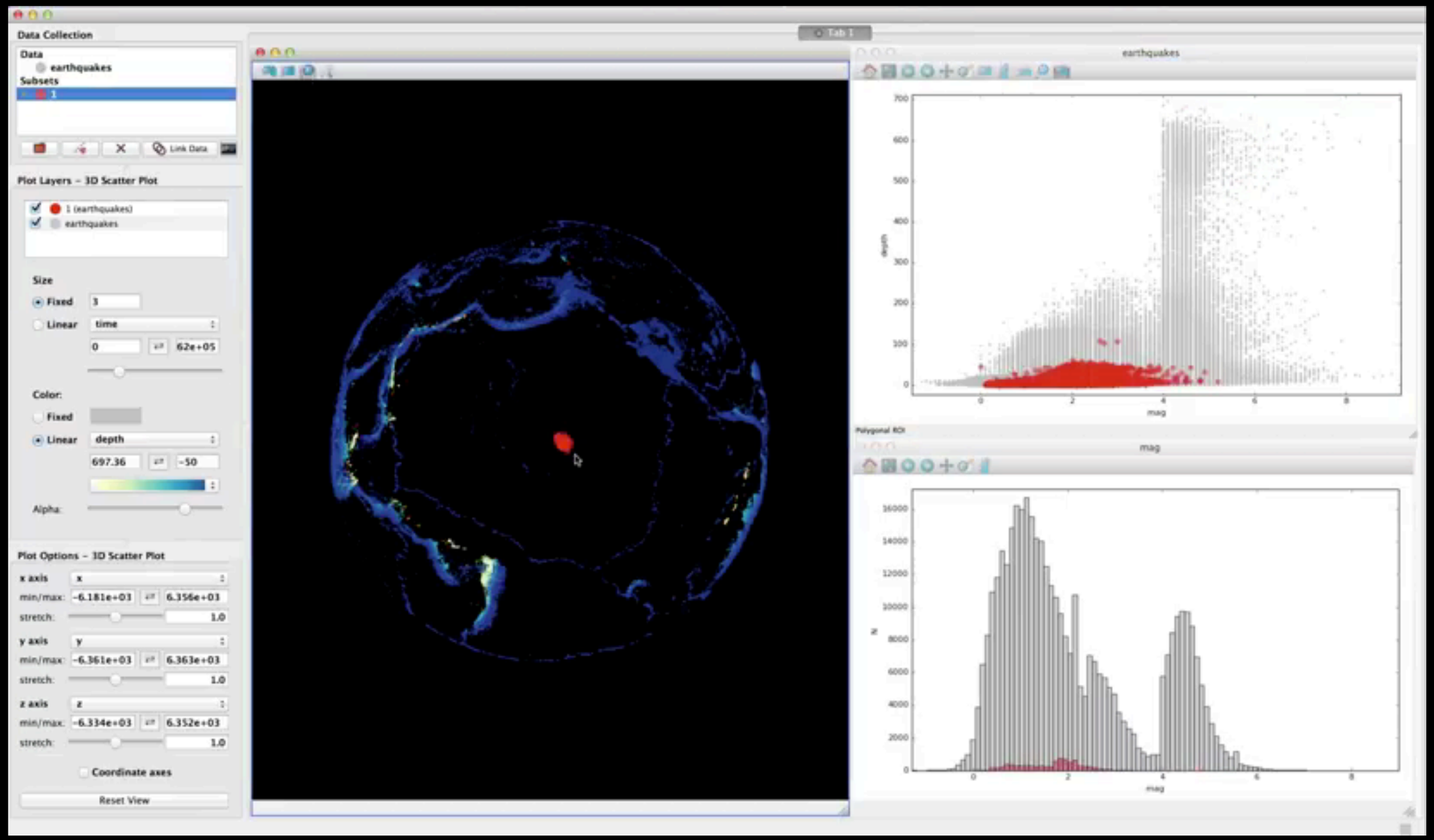

video by Tom Robitaille, lead glue developer

glue created by: C. Beaumont, M. Borkin, M. Breddels, T. Robitaille, C. Zucker, and A. Goodman, PI

PERSEUS in glue

python File Edit View Canvas Data Manager Plugins Help — 20% Mon Oct 22 7:15 AM Alyssa A Goodman

Glue

Open Session | Export Session | Import Data | Export Data/Subsets | Link Data | Arithmetic attributes | Active Subset: Subset 3 | Mode: | Terminal | Preferences | Error Console

Data Collection

Data
- PerA_12coFCRAO_F_xyv
- PerA_13coFCRAO_F_xyv
- Perseus_Av_NICER
- PerA_AvTemMIPS_F_Av
- PerA_AvTemMIPS_F_T
- Perseus_fcrao_iras_2mass

Subsets
- spec_probe
- hot_highv
- Subset 3

Plot Layers - 2D Scatter
- Subset 3 (Perseus_fcrao_iras_2mass)
- hot_highv (Perseus_fcrao_iras_2mass)
- spec_probe (Perseus_fcrao_iras_2mass)
- Perseus_fcrao_iras_2mass

Color | Points | Line | Errors | Vectors

color: Fixed

opacity

Plot Options - 2D Scatter

General | Limits | Axes

x axis: V13CO log

y axis: TIRAS log

COMPLETE
data in glue

Tab 1 | Tab 2

2D Image

2D Scatter

Dec vs RA

1D Profile

Data values vs Velocity

2D Scatter

TIRAS vs V13CO

3D Scatter

NIRAS vs Dec vs RA

+plug-ins, now: OpenSpace & in-prep: ALADIN esa Sky yt

glue
multidimensional data exploration
glueviz.org

glue solutions inc. gluesolutions.io

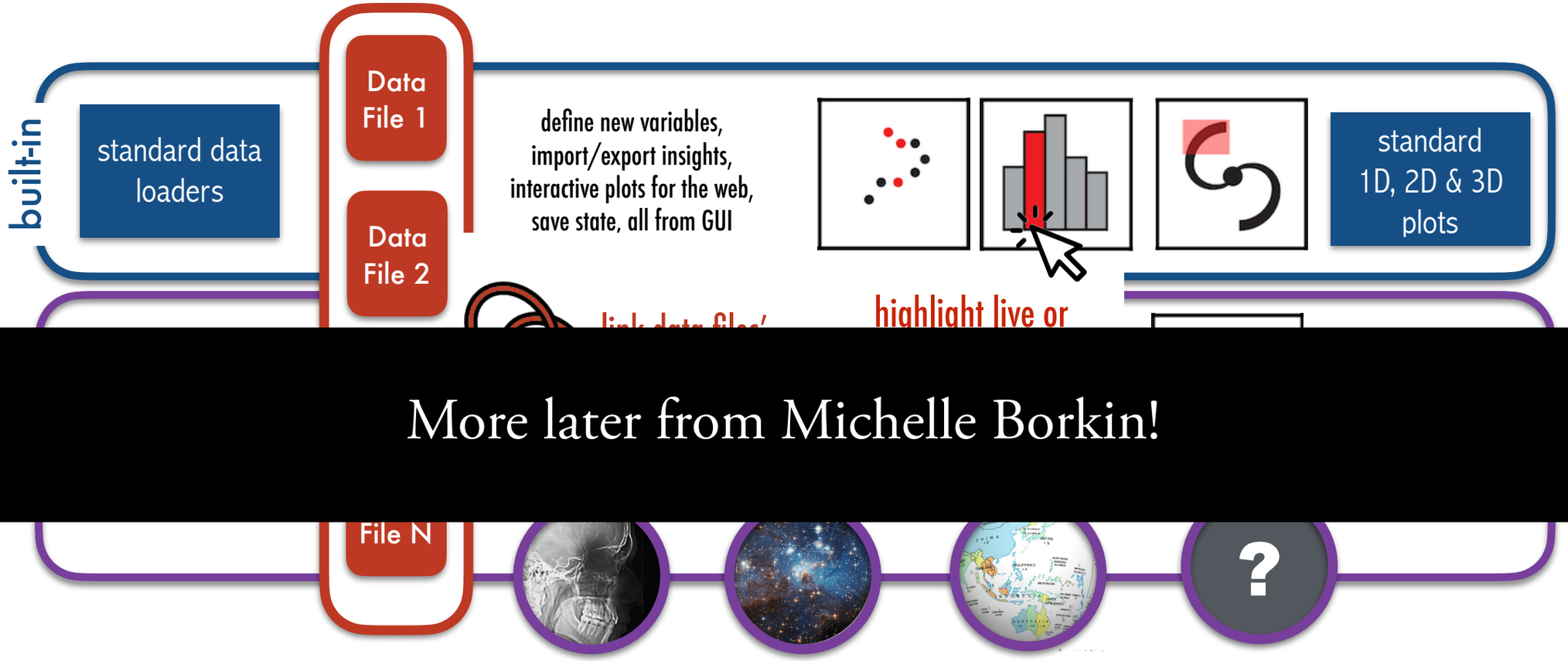

More later from Michelle Borkin!

+plug-ins, now: OpenSpace & in-prep: ALADIN esa Sky yt

Our Universe is not two-dimensional, but the Sky is.

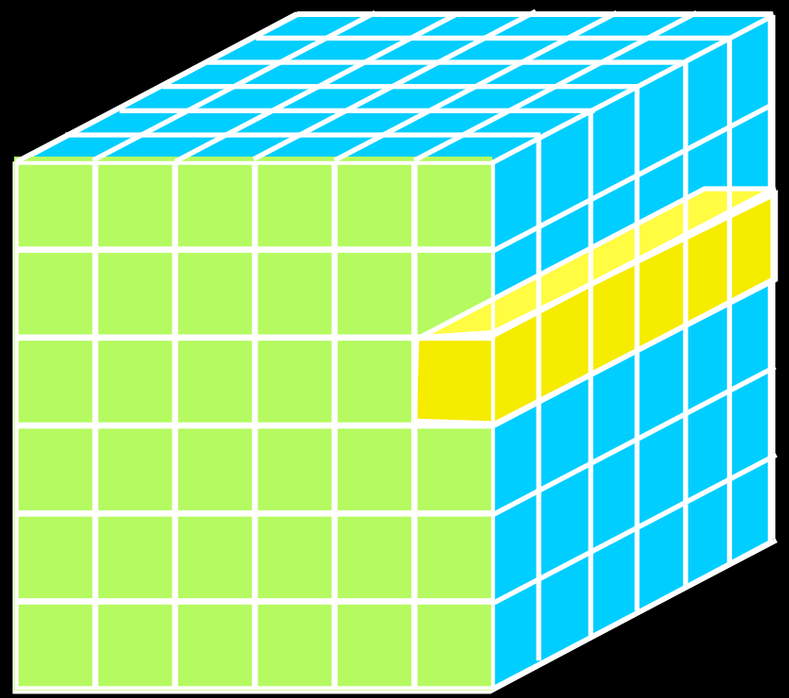

"DATA, DIMENSIONS, DISPLAY"

1D: Columns = “Spectrum”,“Time Series,” “Sequence”
2D: Faces or Slices = “Images,” “Arrays”
3D: Volumes = “3D Renderings”, “2D Movies”
4D: Time Series of Volumes = “3D Movies”

Sculpture

Sfumato

Sfumato

"Astronomy Picture of the Day" for 24 October 2020

© KIPAC, AMNH

Sfumato? SCULPTURE?

Both? Neither? The brain is (well) fooled by the combination motion & occlusion.

Note importance of memory, though…

Dark Matter Pre-Visualization for AMNH "Dark Universe" Space Show

from collaboration of Kaehler, Abel, Emmart, MacLow, Hahn 2014

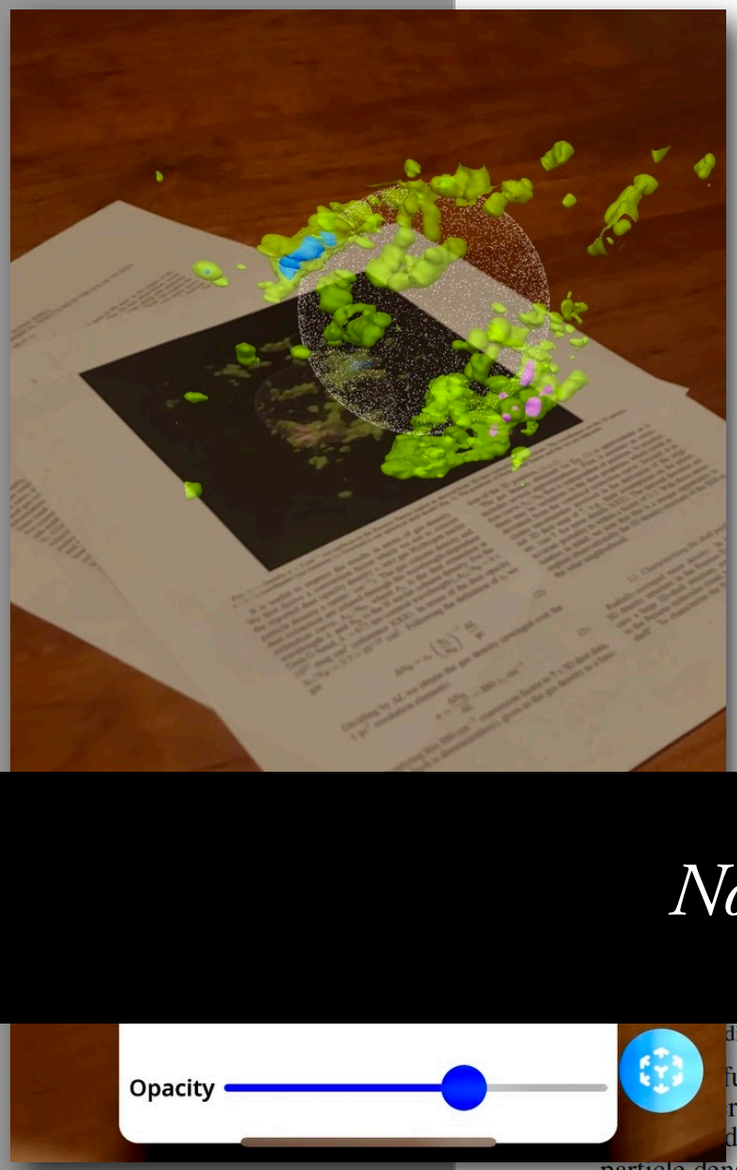

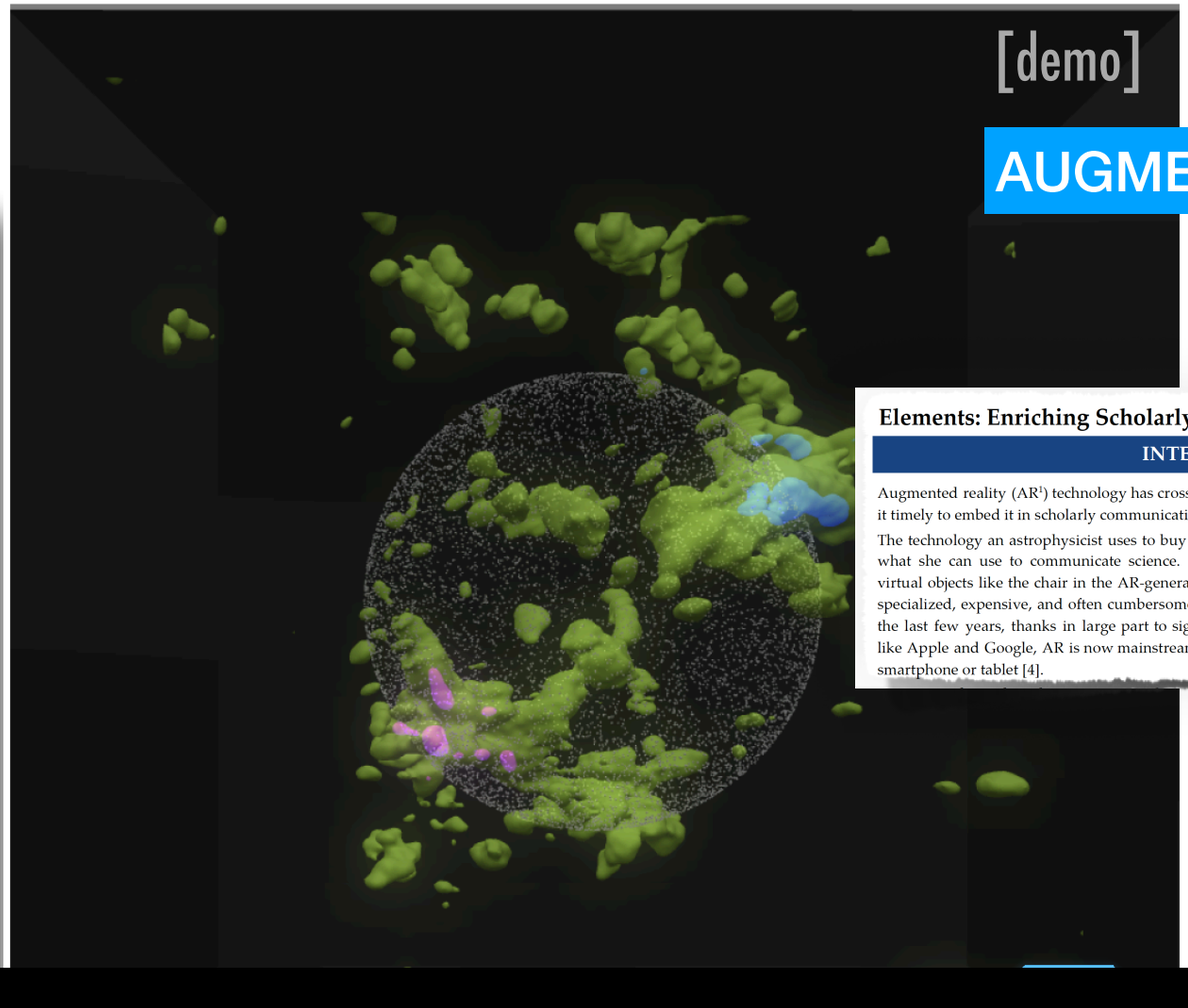

AUGMENTED REALITY(!)

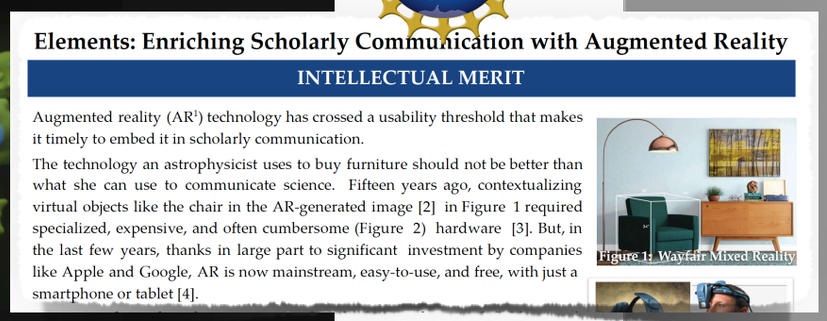
Elements: Enriching Scholarly Communication with Augmented Reality

INTELLECTUAL MERIT

Augmented reality (AR[1]) technology has crossed a usability threshold that makes it timely to embed it in scholarly communication.

The technology an astrophysicist uses to buy furniture should not be better than what she can use to communicate science. Fifteen years ago, contextualizing virtual objects like the chair in the AR-generated image [2] in Figure 1 required specialized, expensive, and often cumbersome (Figure 2) hardware [3]. But, in the last few years, thanks in large part to significant investment by companies like Apple and Google, AR is now mainstream, easy-to-use, and free, with just a smartphone or tablet [4].

Note importance of memory, though…

Excerpt from Bialy, Zucker, Goodman, et al. in prep

dinates (see footnote 1). Ov

ful to express the res
rive a conversion fac
d dust opacity density
particle density n (units: cm^{-3}).
dust extinction are related throug
extinction curve, $A_\lambda/N_{\rm H}$, where
wavelength λ and $N_{\rm H}$ is the H nu
Gaia G-band, $\lambda = 673$ nm (centra
10^{22} mag cm^2 (reference XXX).
$\tau_{\rm G}/N_H = 3.7 \times 10^{-22}$ cm^2. Foll
get

$$\Delta N_{\rm H} = s_x \left(\frac{\tau_{\rm G}}{N_{\rm H}} \right.$$

Dividing by ΔL we obtain the ga
1 pc^3 resolution element):

$$n = \frac{\Delta N_{\rm H}}{\Delta L} = 88$$

Figure 7: Screenshots from demo (video) for Hanaheia AR Figure from an upcoming AAS Journal article

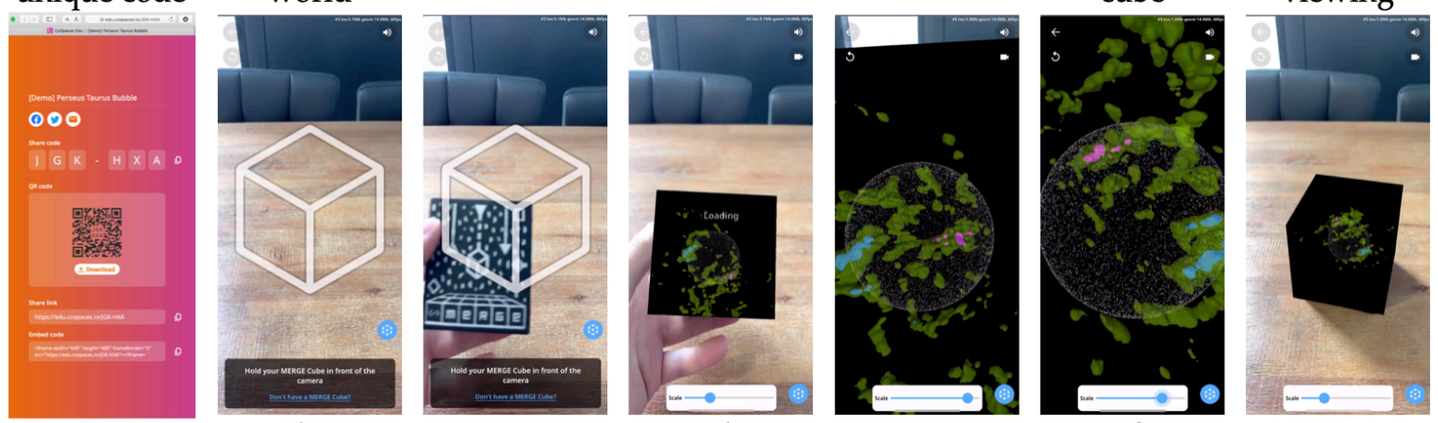

COLLABORATION

EXPLANATORY VISUALIZATION

citizen science

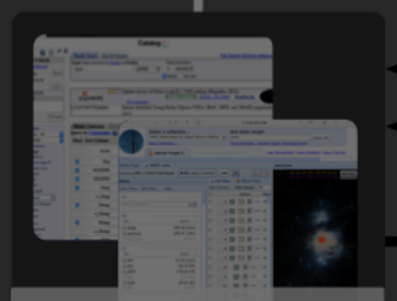

shared data

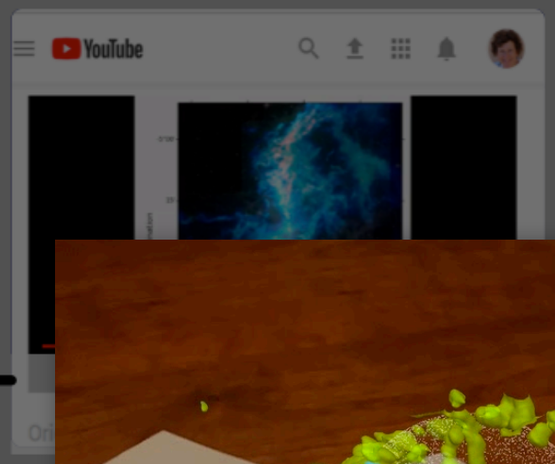

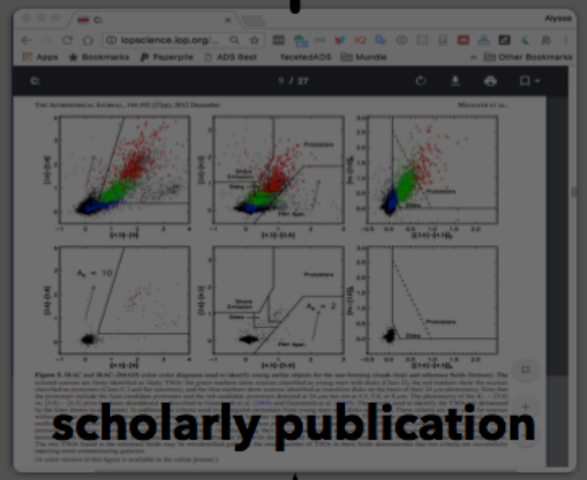

scholarly publication

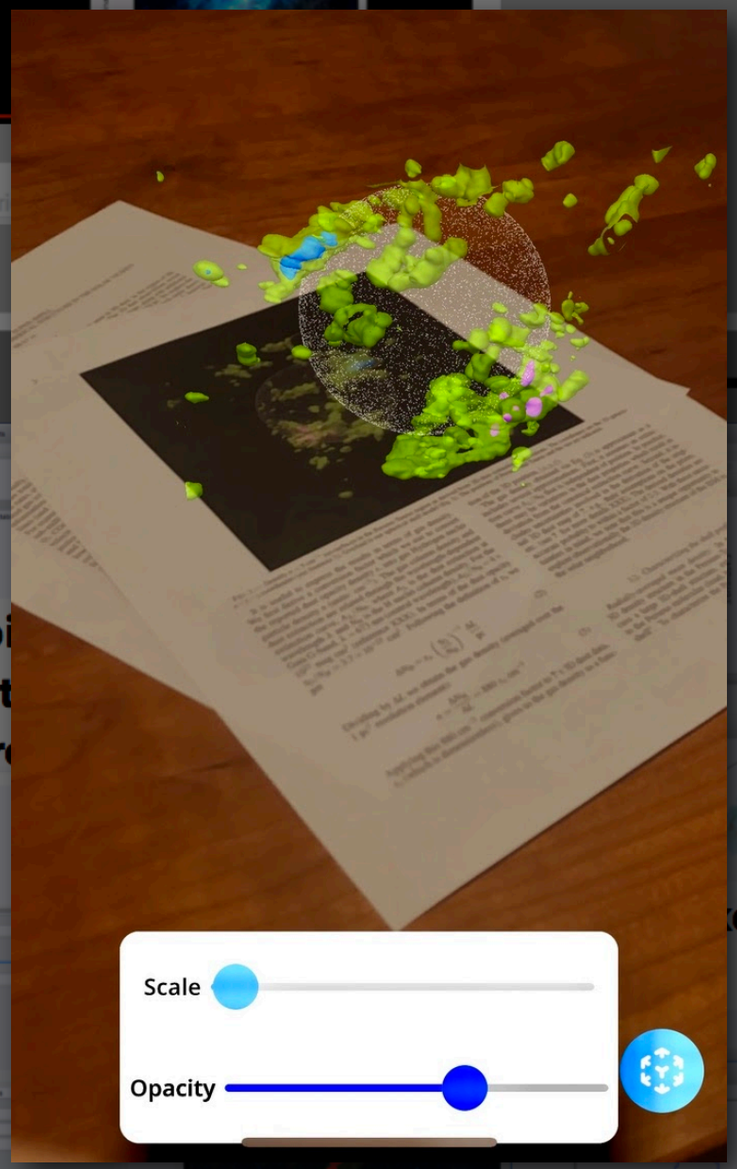

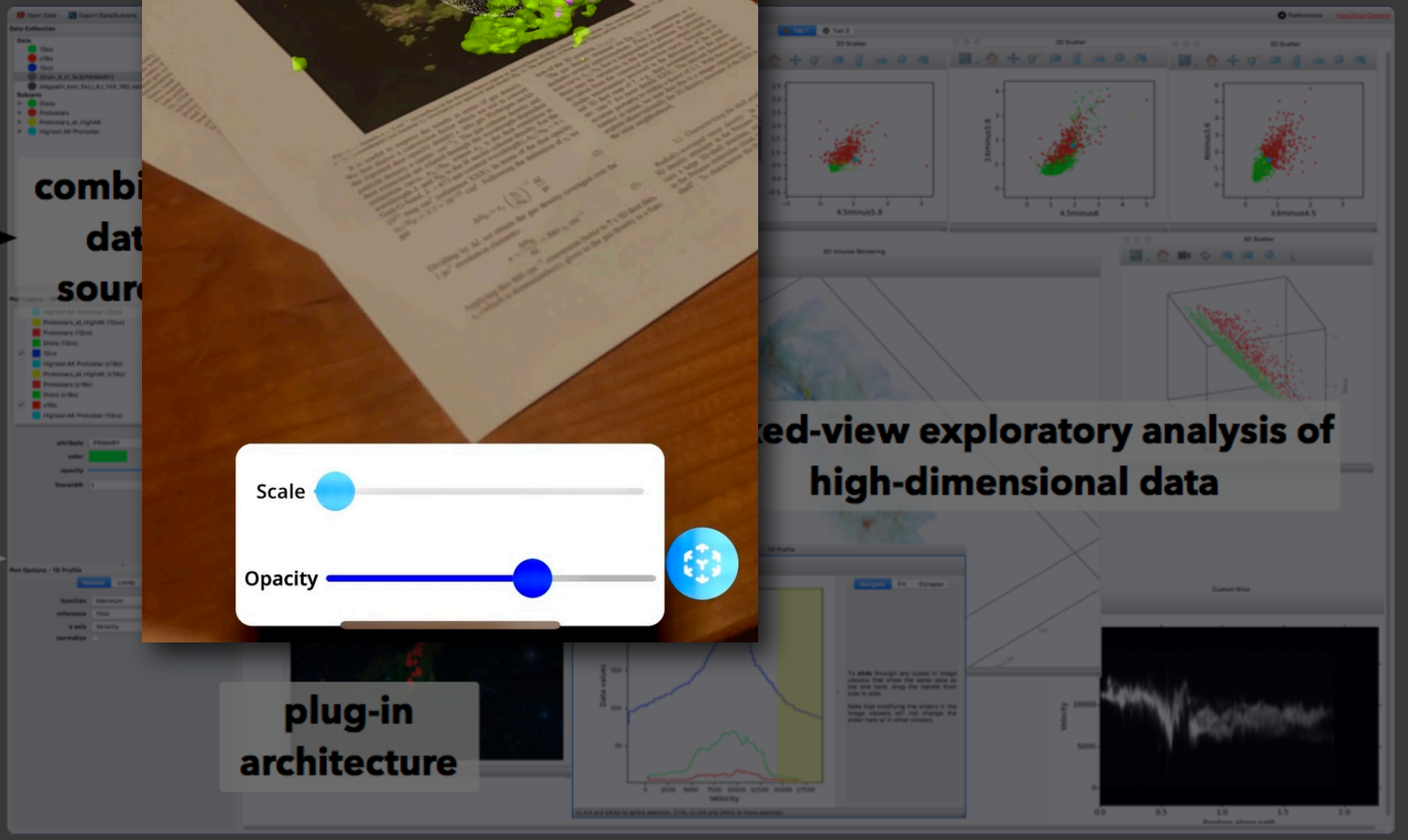

combi
dat
sour

plug-in architecture

ed-view exploratory analysis of high-dimensional data

open source, modular, software

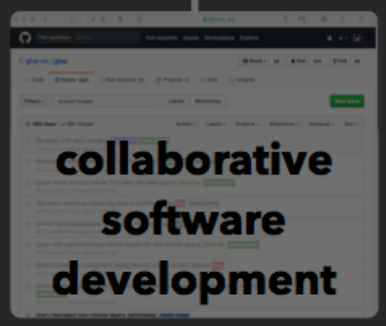

collaborative software development

EXPLORATORY VISUALIZATION

COLLABORATION

EXPLANATORY VISUALIZATION

citizen science

shared data

public outreach

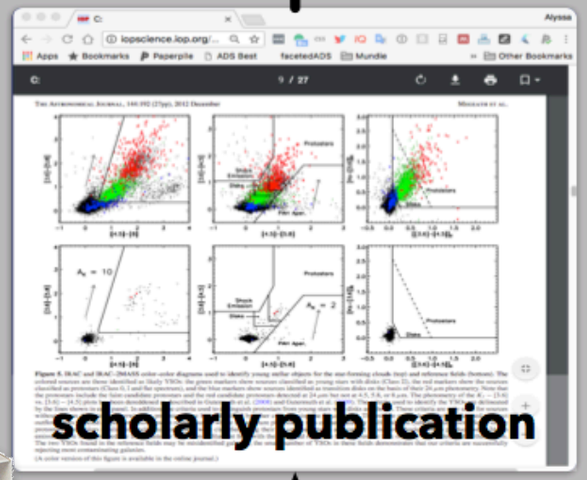

scholarly publication

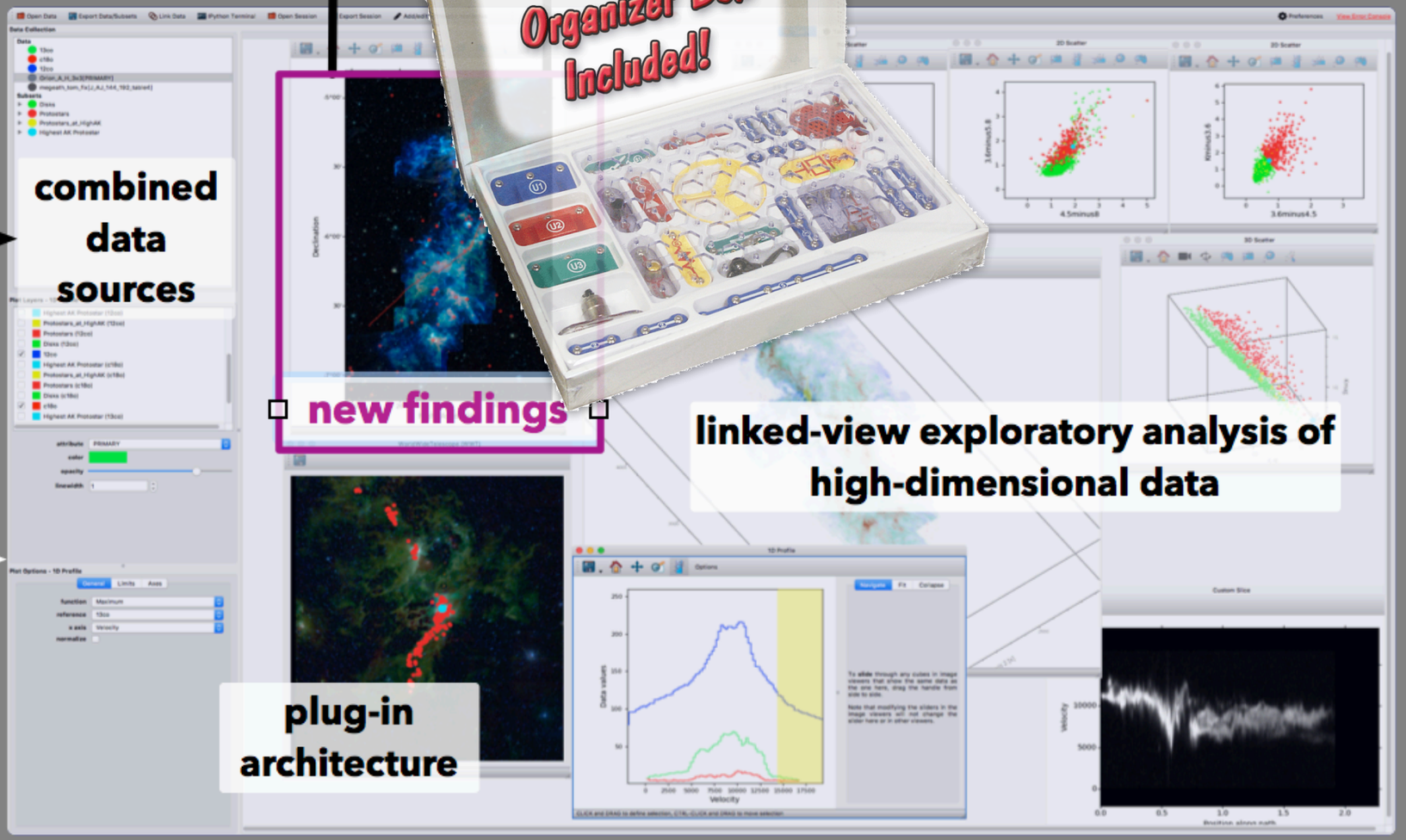

combined data sources

new findings

linked-view exploratory analysis of high-dimensional data

open source, modular, software

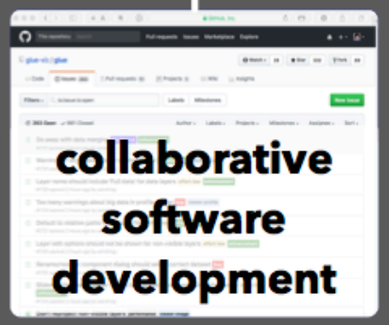

collaborative software development

plug-in architecture

EXPLORATORY VISUALIZATION

[demo]

The Radcliffe Wave

VISUALS

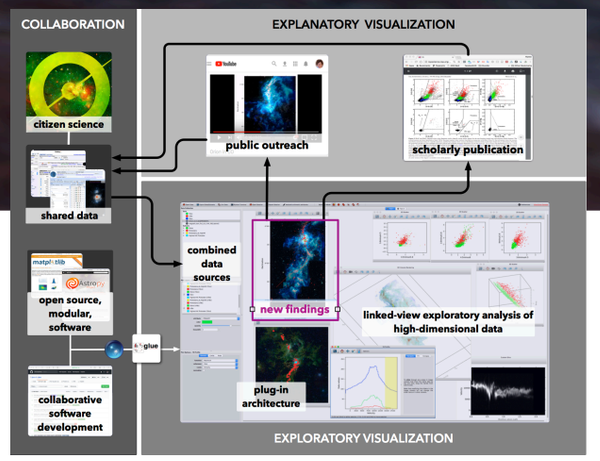

On this page: INTERACTIVES, FIGURES, VIDEOS -- scroll down to see it all.

INTERACTIVES

Explore the RadWave in 3D

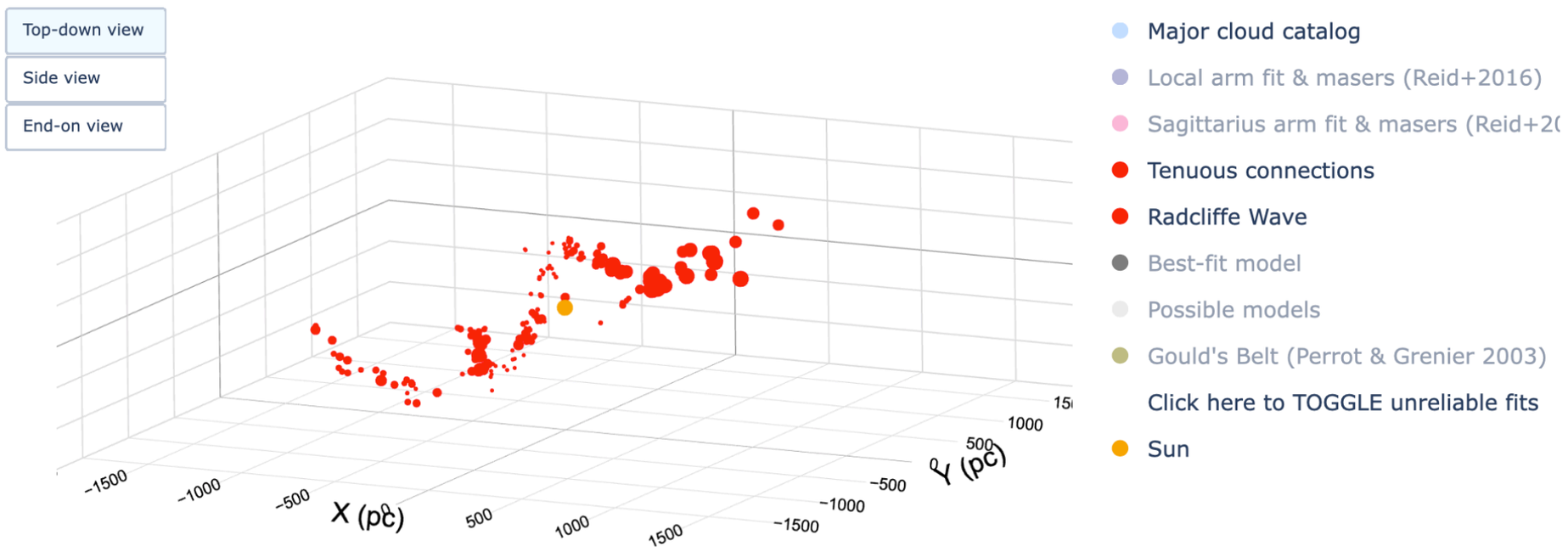

The same tools can work for research, teaching & outreach.

10QViz.org

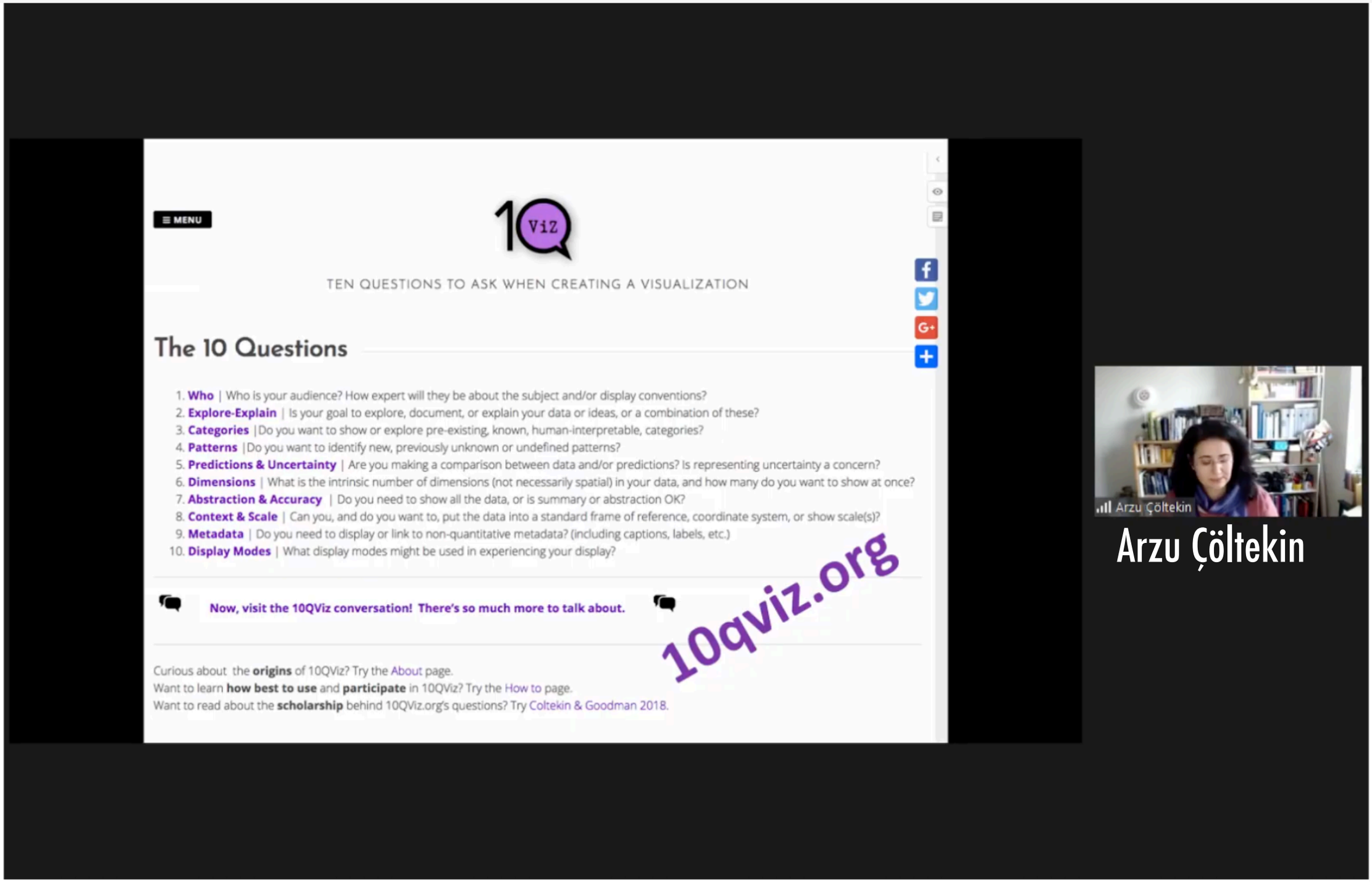

Benjamin Bach, Sheelagh Carpendale, Arzu Coltekin, Robert S. Laramee, Lace Padilla, Jonathan Roberts - Panel 1: Teaching Visualization Guidelines

Our Universe is not two-dimensional, but the Sky is.

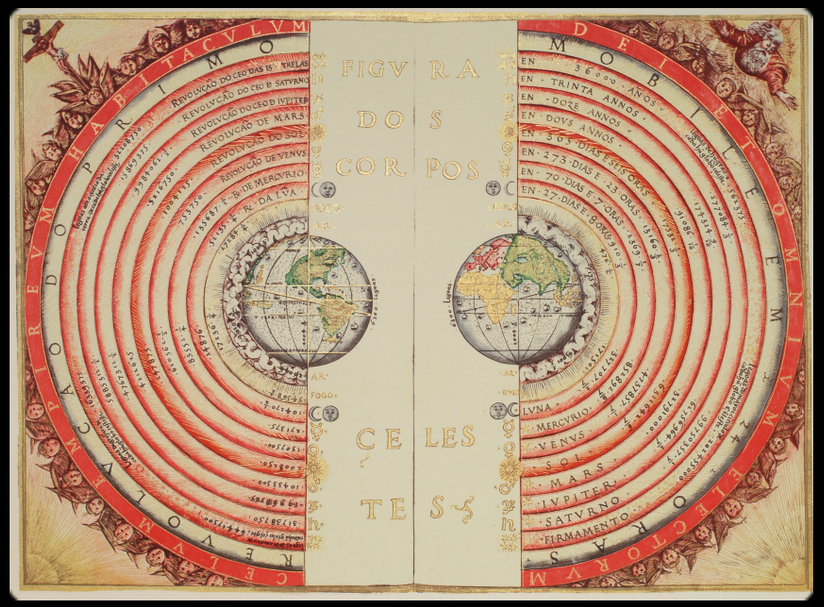

100 AD–16th Century

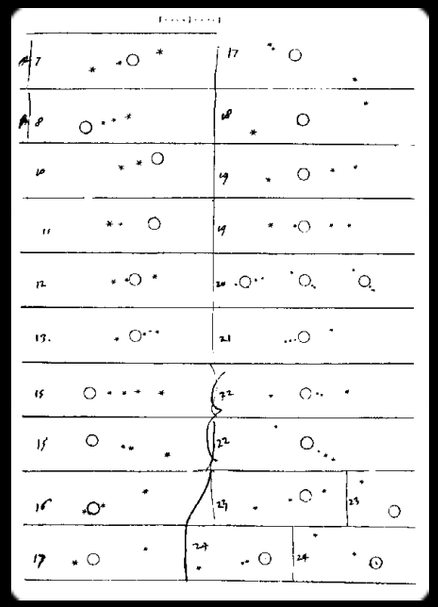

17th Century

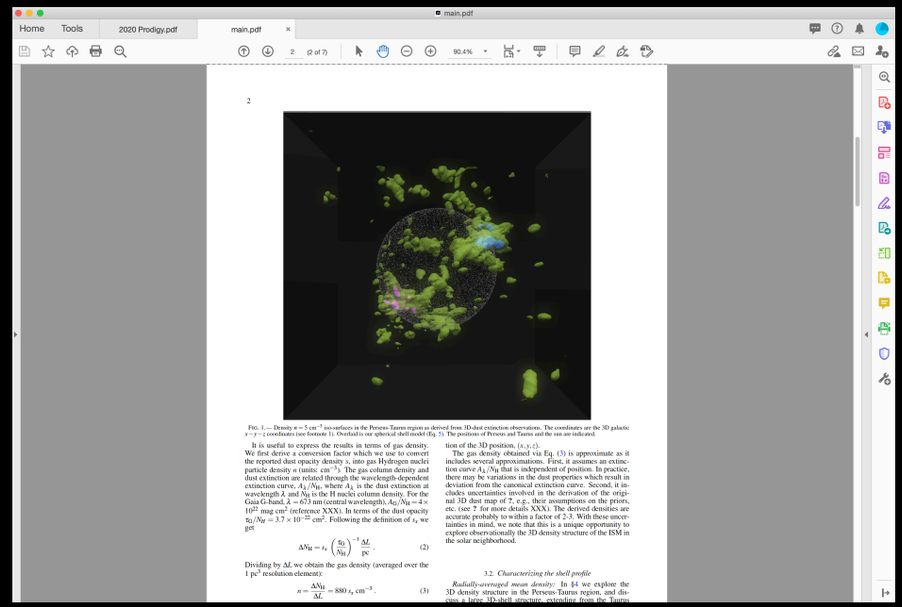

21st Century

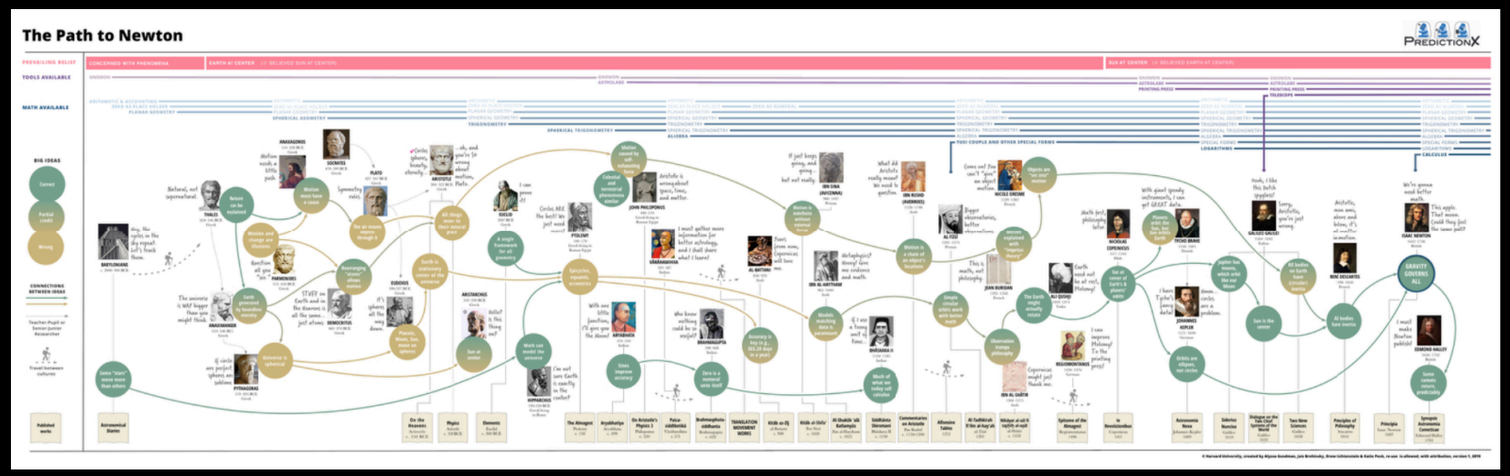

"The Path to Newton"

100 years of Perseus

+2 Challenges...

"case" as a variable...

3D selection

tinyurl.com/AGVisIEEE20

The Past, Present and Future of Visualization in Astronomy

Alyssa A. Goodman *(and MANY others!)*

Center for Astrophysics | Harvard & Smithsonian, Radcliffe Insitute for Advanced Study, HDSI Steering Committee & glue solutions, inc.

@AlyssaAGoodman

© KIPAC, AMNH

This document is online at tinyurl.com/AGVisIEEE20

Links & Pointers from Alyssa Goodman's IEEE Vis 2020 Talk on

"The Past, Present and Future of Visualization in Astronomy"

[at Visualization in Astrophysics Workshop]

[Talk slides on iCloud, *modulo* missing fonts, download for a better experience]

glue: multi-dimensional linked-data exploration

World Wide Telescope, WorldWide Telescope Ambassadors STEM Outreach Program

ADS All-Sky Survey, Aladin, ESA Sky

The Path to Newton, PredictionX

The Timeline Consortium, Aeon Timeline, HarvardX , edX, LabXChange,

OpenSpace, astropy, yt

glue solutions, inc. (consulting)

AR Demos (scan AR codes with mobile device, right-hand code requires a Merge Cube)

"Perseus" progress

2008

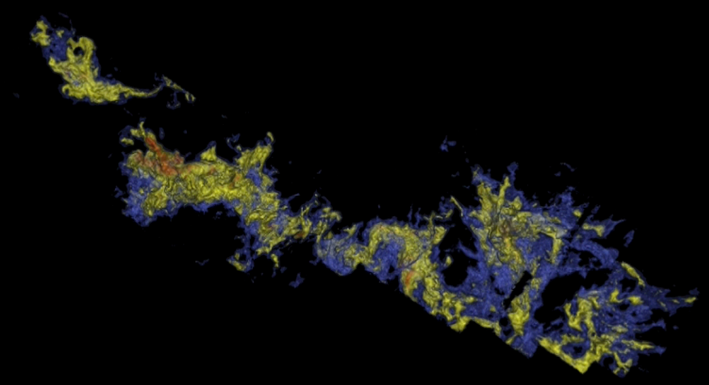

2009

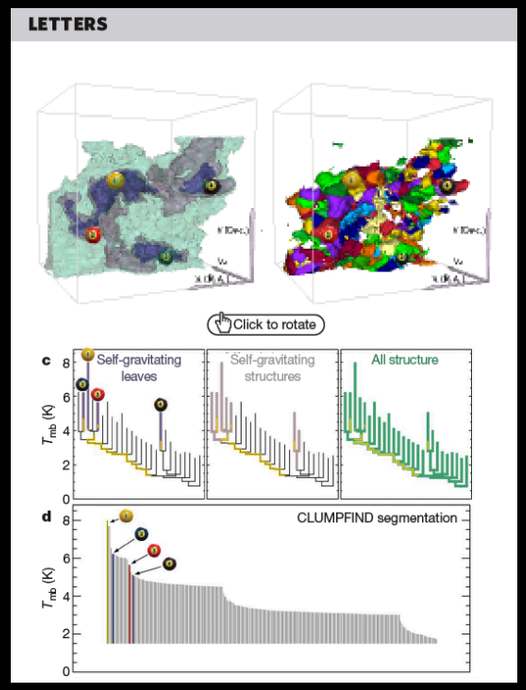

2012

glue
multidimensional data exploration

2015

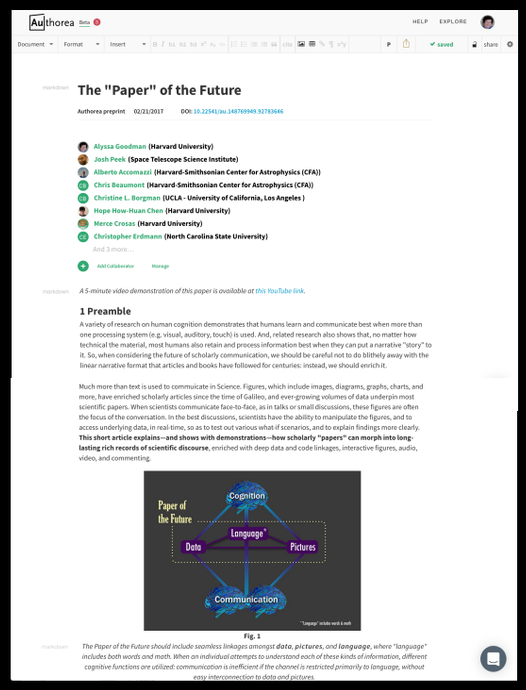

2018

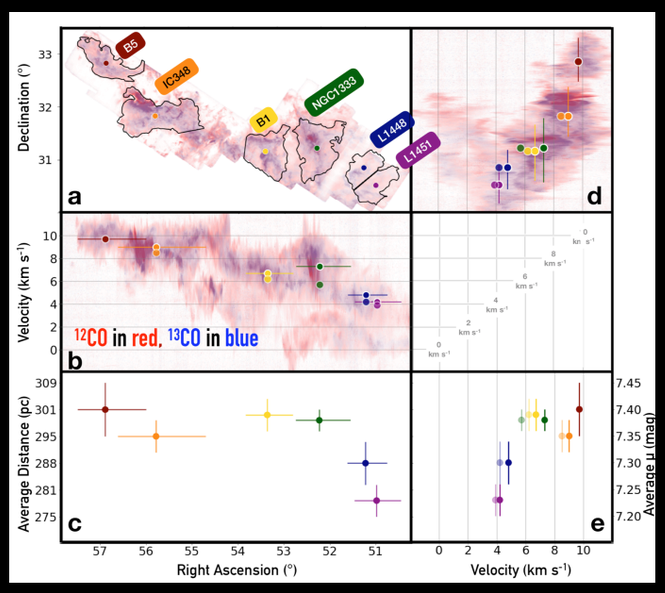

2020

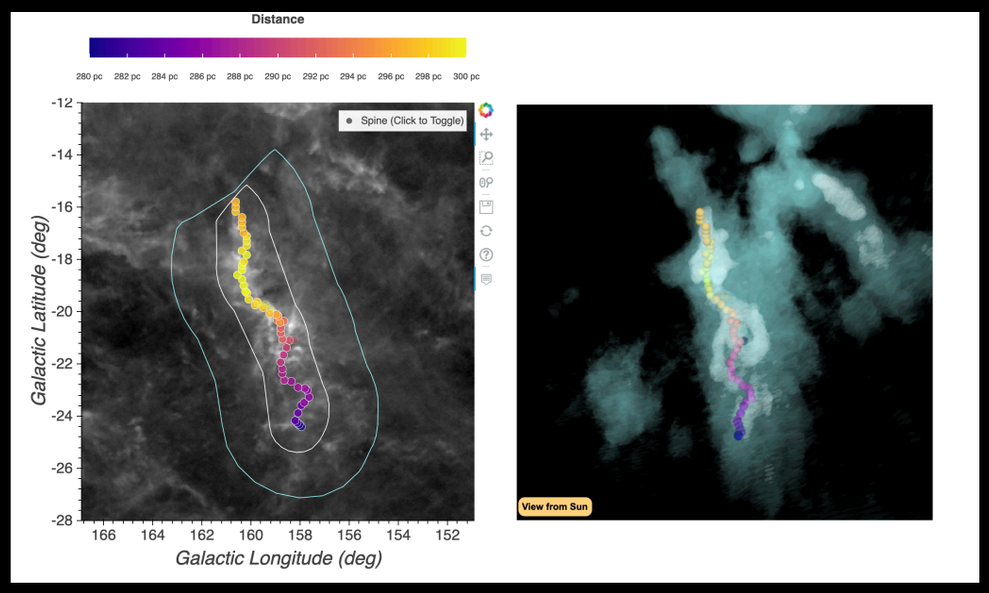

2020+

VBB
PZL

"Perseus" Progress

AEON TIMELINE

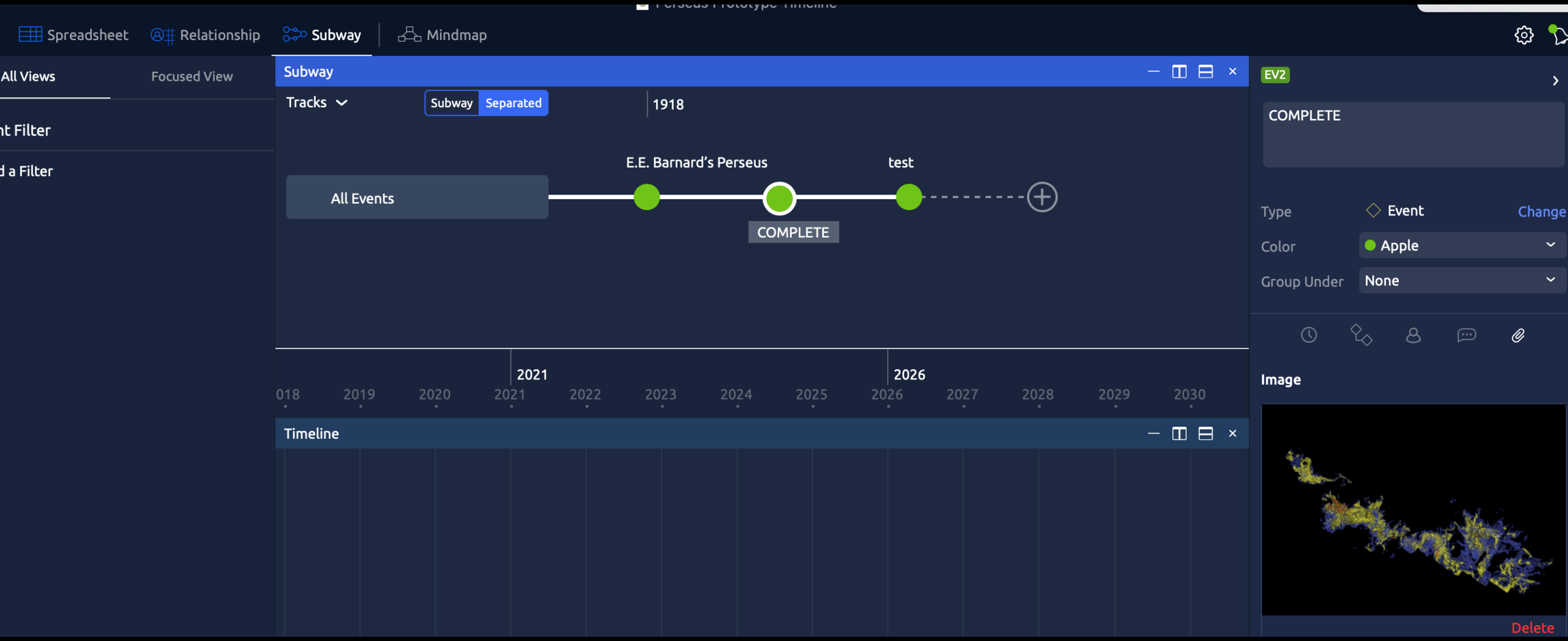

[coming soon!]

“Dimension” isn’t even always spatial…
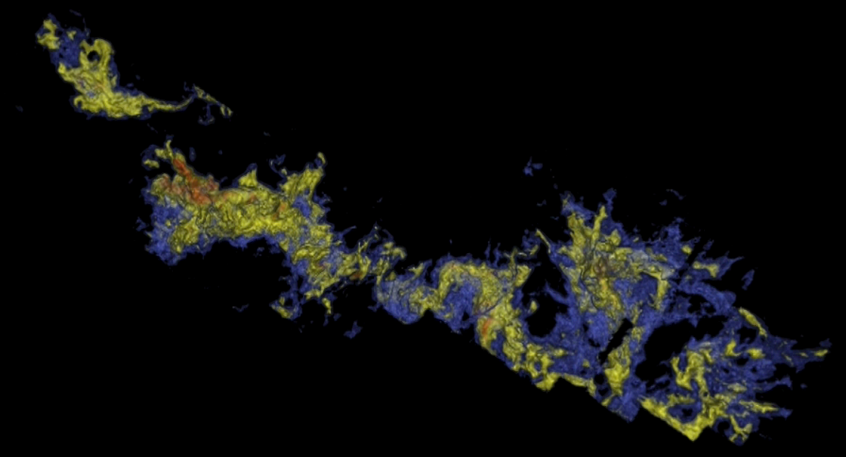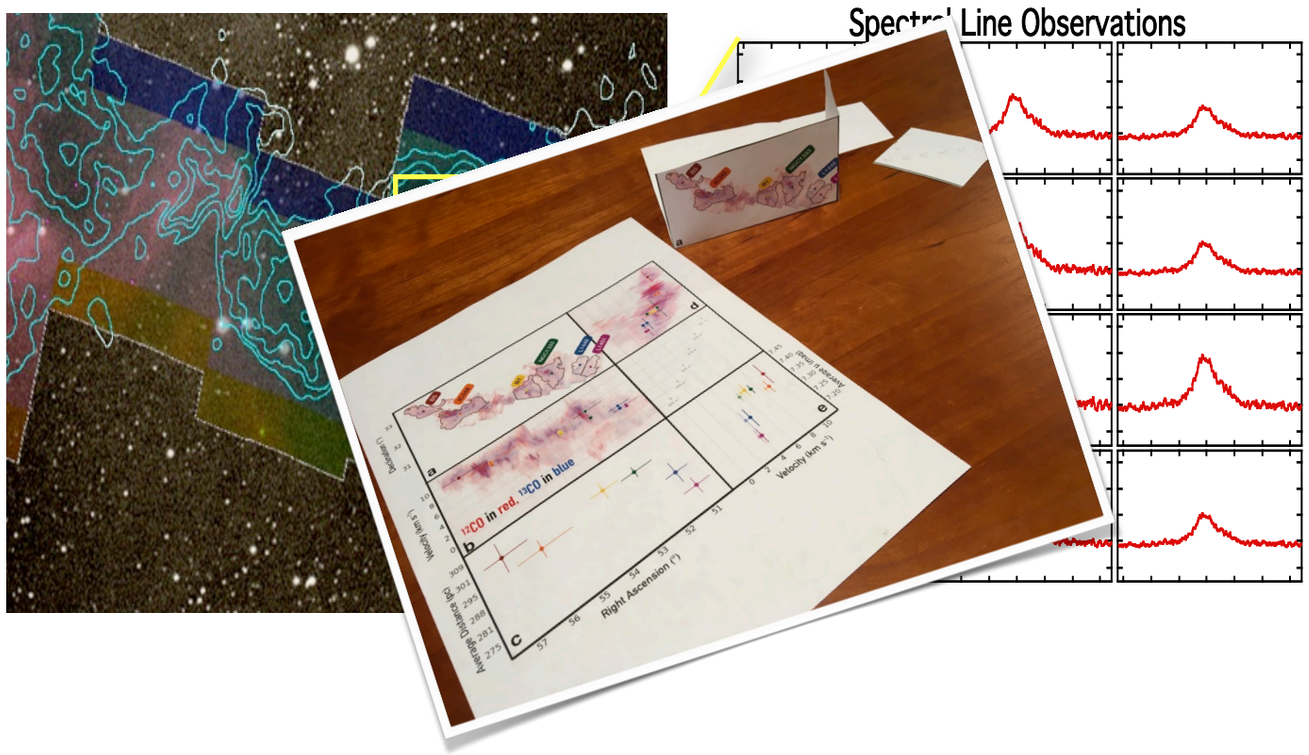
The “3rd” dimension in this 3D plot is “velocity” coming from Doppler Spectroscopy.